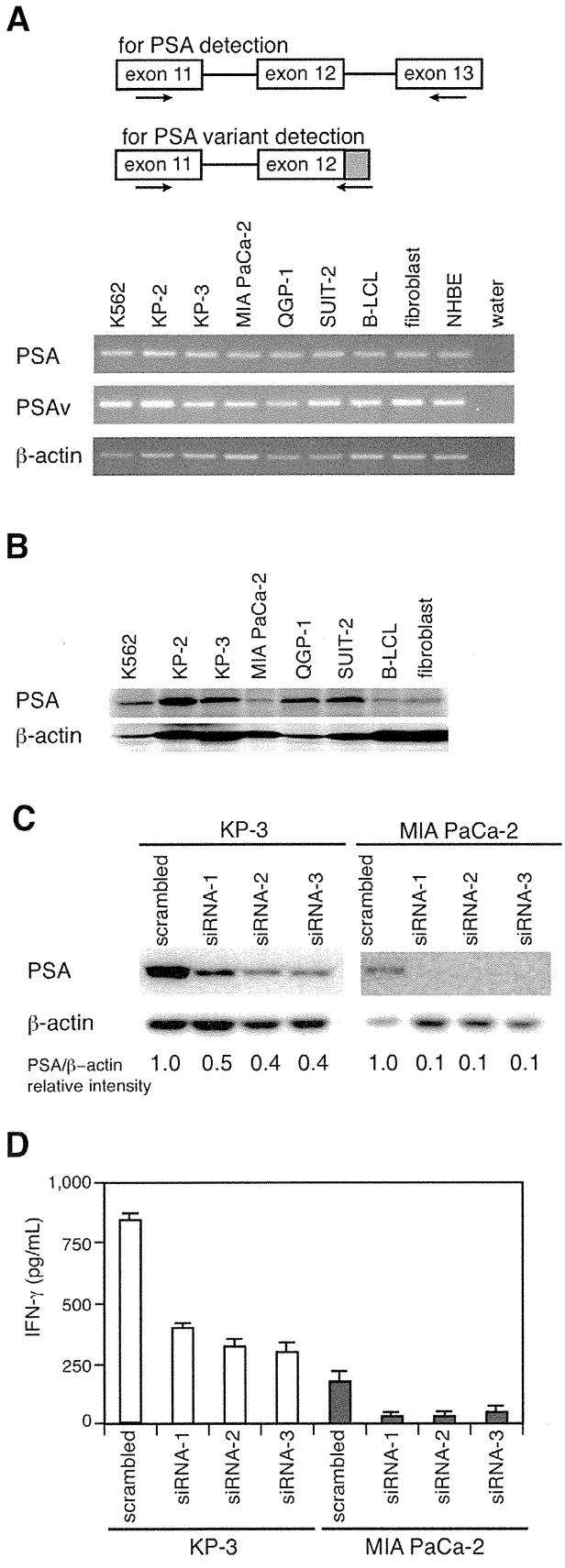

Figure 2. Ubiquitous expression of the PSA mRNA and protein within various cells irrespective of clone recognition. A, Two RT-PCR primer sets are designed to discriminate between wild type and variant PSA (PSAv), indicated by horizontal arrows (top). RT-PCR analysis was performed using the PSA primer sets and those for β-actin (bottom). B, The expression of the PSA and β-actin proteins was analyzed using Western blot analysis. C, KP-3 and MIA PaCa-2 cells were transfected for 70 h with scrambled or PSA-specific siRNA. Three different siRNA targets were chosen for the PSA gene, and Western blot analysis of the PSA protein in siRNA-treated cells was performed. The intensities of the bands were calculated using the ImageJ software. D, CTL responses against siRNA-treated cells were examined using an IFN-γ ELISA. The results are expressed as the means ± SD of triplicate values. Similar results were obtained in three separate experiments.
doi:10.1371/journal.pone.0047126.g002

Discussion

The present study demonstrated, using cDNA expression cloning, that a variant PSA was an antigen recognized by 16F3, although full-length PSA also stimulated 16F3. Remarkably, despite the ubiquitous expression of both the variant and full-length forms, the 16F3 CTL was found preferentially to recognize cancer cells but not normal cells. As other examples of this phenomenon, transcripts of p15 and cDNA31.2 are ubiquitously expressed, yet relevant CTLs only recognize tumor cells and not normal cells, including B-LCLs [26,27]. Herein, we demonstrate a new mechanism of antigen processing and presentation that emphasizes the differences between cancer and normal cells with respect to ubiquitously expressed proteins. Based on the present results with specific inhibitory chemicals and siRNA targeting autophagy, and monitoring the results of autophagic activities, epitope liberation is caused by differences in the autophagic status, and therefore, a ubiquitously expressed protein, PSA, mimics tumor-associated antigens through a unique mechanism involving autophagy.

Our data indicate that both autophagosomes and proteasomes are necessary for the processing of the epitope peptide from PSA. Taking into consideration that lactacystin considerably decreases PSA epitope presentation to CTLs (Figure 3B) without changing the level of full-length PSA protein (Figure 6C), it is likely that proteasomes cleave smaller fragments of PSA to create the epitope. We speculate that these data suggest that PSA is degraded through the autophagosome-lysosome pathway prior to digestion in the proteasome.

Autophagy plays an important role in tumor initiation and progression in contrasting manners. Cancer cells use autophagy to survive and propagate in hypoxic and low-nutrient microenvironments, whereas autophagy is suppressive of tumor initiation because of the clearance of mutations. Increased autophagy has been shown in late-stage colon cancer [28], breast cancer [29], melanoma [30], hepatoma [31] and malignant glioma [32]. Additionally, for pancreatic cancer, autophagy correlates with a poor outcome [33] and is required for tumor growth [34]. Moreover, autophagy is associated with mutated K-ras-induced malignant transformation [35,36]. Taken together, most pancreatic cancer cells with a K-ras mutation at codon 12 should have constitutively active autophagy. We demonstrated that an autophagosomal marker LC3 was strongly expressed in KP-3 and MIA Paca-2 cells. These pancreatic ductal cancer cell lines have a K-ras mutation at codon 12, whereas autophagosome is basal level in KP-2 cells having no K-ras mutation [37]. Remarkably, rapamycin treatment and starvation did not induce normal fibroblast cells to create the epitope, although autophagosome was observed. Our data suggest that aberrant increases in autophagosomes in association with K-ras mutation create distinct peptide repertoires displayed on the MHC class I molecules of

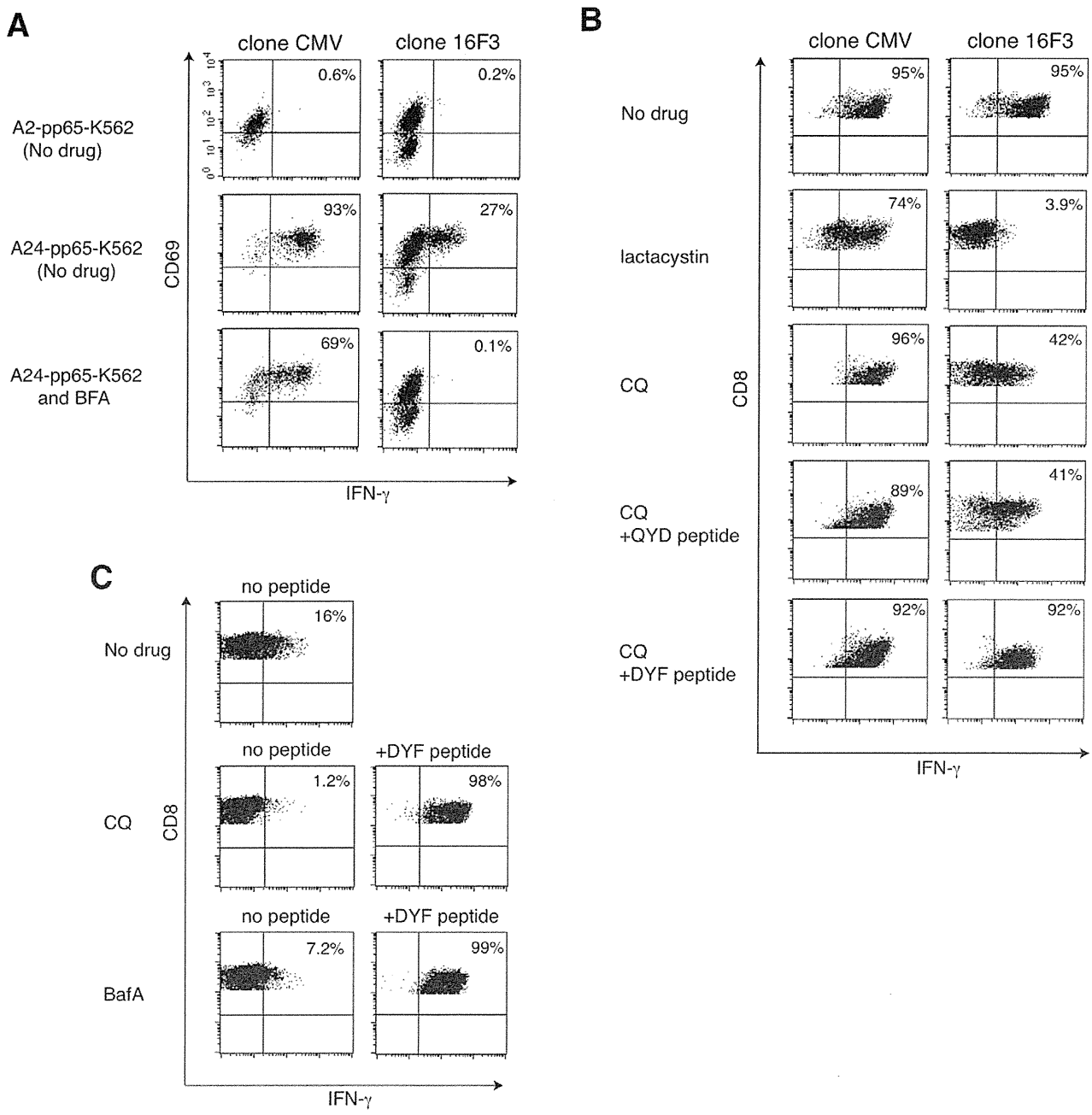

Figure 3. The epitope is presented and processed through a vacuolar pathway. A, K562 cells expressing both HLA-A2 or A24 and CMV pp65 (A2-pp65-K562 or A24-pp65-K562) were acid-stripped and incubated at 37°C for 9 h in the presence or absence of BFA. Then, the cells were co-cultured with either 16F3 or an HLA-A24-restricted CMV pp65-specific CTL clone for an additional 5 h. BFA was also added during the co-culture. After fixation and permeabilization, the cells were stained for CD3, CD8, CD69 and IFN-γ. $CD3^+$ and $CD8^+$ T cells were gated and analyzed using a flow cytometer. The frequency of IFN-γ producing cells is shown as the percentage of the total $CD3^+$ $CD8^+$ T cells. B-C, IFN-γ secretions of clones for 4 h after stimulation with A24-pp65-K562 cells (B) or KP-3 cells (C) treated with acid buffer for peptide stripping and/or inhibitors for 14 h was detected using an IFN-γ catch assay. 7-AAD^- alive $CD8^+$ T cells were gated and analyzed using a flow cytometer. The frequency of IFN-γ secreting cells is shown as the percentage of the total alive $CD8^+$ T cells. Whereas irreversibly acting lactacystin was removed during co-culture period (B), CQ and Baf A were retained in the media (B, C) because of their reversible nature. To exclude the possibility that CQ and Baf A could be inhibitory for 16F3 to produce IFN-γ, cognate or irrelevant peptides were added at concentrations of 1 μg/ml (B, C) and the T-cell response was examined.
doi:10.1371/journal.pone.0047126.g003

cancer cells, potentially evoking CTL responses while sparing normal cell damage.

In this study, a long 12-mer epitope antigen derived from PSA was identified, consistent with an earlier investigation that revealed an unusually long epitope presented on MHC class I [38]. Not only viral antigens but also tumor antigens are naturally processed into longer epitopes, and higher immunogenicities are indicated even in cancer patients [39]. The structures of the long peptides on

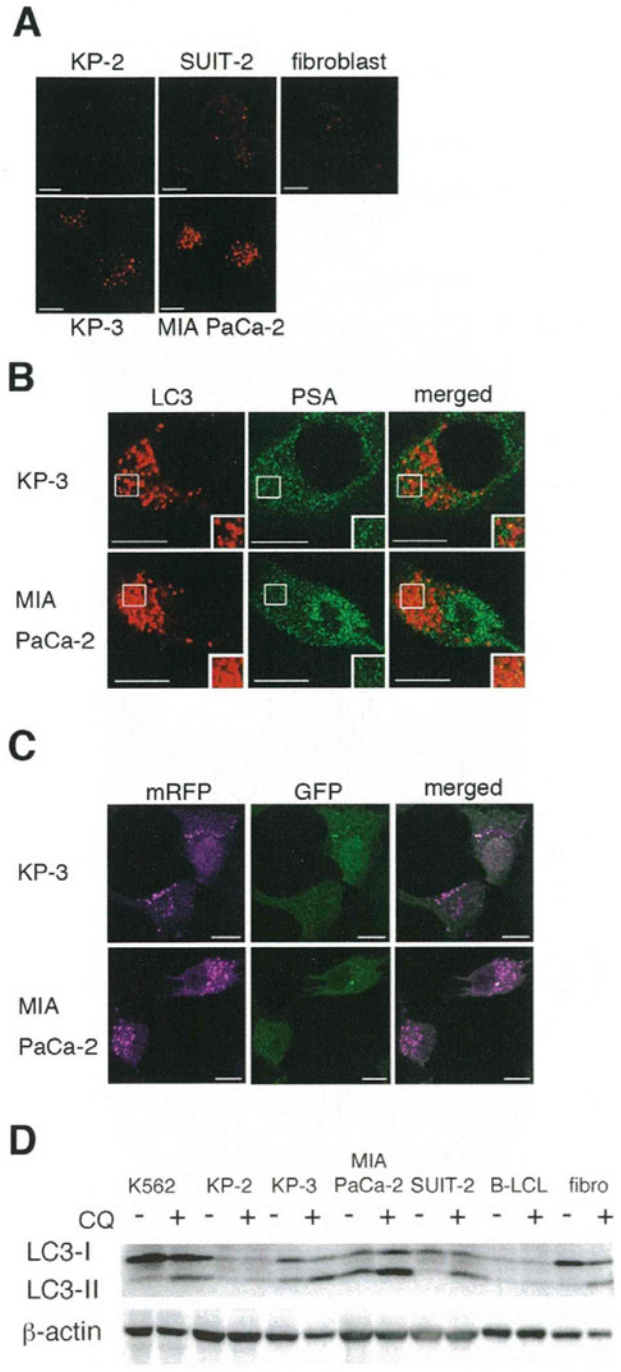

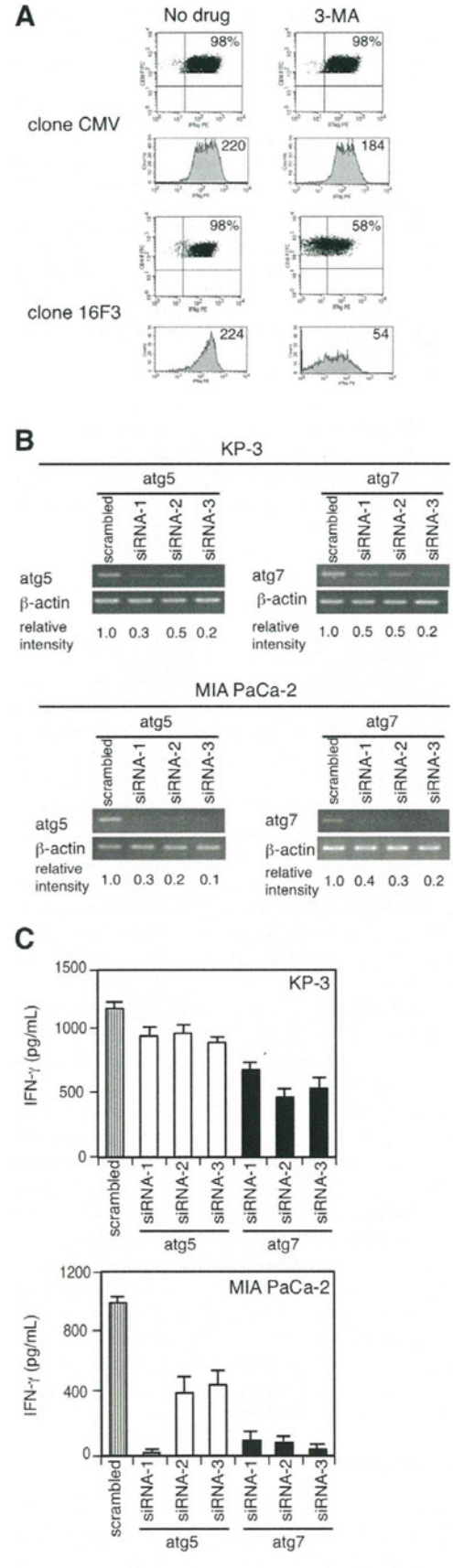

Figure 4. Constitutively active autophagy is involved in the 16F3 epitope processing of cancer cells. A, An immunofluorescence assay was performed to examine the expression of endogenous LC3. B, Double staining for endogenous LC3 and PSA was performed. Cells were cultured with BafA for 4 h, and then immunocytochemistry was performed. A yellow signal indicates colocalization. C, KP-3 and MIA PaCa-2 cells were transfected with plasmids expressing an mRFP-GFP-LC3 tandem-tagged fluorescent protein. Forty hours after transfection, the cells were fixed and analyzed via microscopy. A white signal indicates colocalization. The bars indicate 10 μm (A–C). D, The status of autophagic flux was measured via the LC3-II expression level. Cells were cultured with or without CQ for 2 h, and then the cell lysates were subjected to Western blot analysis for LC3.
doi:10.1371/journal.pone.0047126.g004

Figure 5. Autophagy is involved in the 16F3 epitope processing in cancer cells. A, K562 cells expressing both HLA-A2 or A24 and CMV pp65 were treated with an acid buffer for peptide stripping and incubated for 14 h in the presence or absence of 3-MA. Next, the cells were co-cultured with each clone for 4 h for IFN-γ secretion detected via the IFN-γ catch assay. The frequency of IFN-γ-secreting cells is shown as the percentage of the total living $CD8^+$ T cells. 3-MA was not added during the co-culture period. In the lower panels, histograms of the IFN-γ signal and their mean fluorescence intensity are shown. B, RT-PCR analysis of scrambled, atg5- or atg7-specific siRNA-treated cells performed 70 h after transfection. The intensities of the bands were calculated using the ImageJ software. C, The CTL response against KP-3 and MIA PaCa-2 cells transfected with scrambled, atg5- or atg7-specific siRNA for 70 h was examined using an IFN-γ ELISA. Three different siRNA targets were chosen for each autophagy-associated gene. The results are the means ± SD of triplicates. Similar results were obtained in three separate experiments.
doi:10.1371/journal.pone.0047126.g005

MHC have been characterized, and bulging conformations have been observed [40]. In particular, HLA-B alleles preferentially bind to peptides over 11 residues in length, rather than to other HLA alleles. In this study, we demonstrated that HLA-A24-binding 12-mer peptides were created by autophagy. The epitope DYFNVPYPLKI has anchor residues for HLA-A24, such as a tyrosine at the second position and an isoleucine at the carboxyl-terminus, assuming a bulged formation in the middle of the epitope peptides. The unique processing pathway through autophagy may generate the long epitope peptide.

Concerning adaptive immunity, the report of autophagy-enhancing endogenous presentation on MHC class I is clearly of interest [13]. HSV type 1 (HSV-1) was found to trigger a vacuolar response that increased the presentation of a peptide derived from HSV-1 glycoprotein B to CTL on MHC class I. In HSV-1-infected murine macrophages, LC3-positive four-layered membrane structures emerged from nuclear envelopes and were uniquely found in "classical" autophagosomes, consisting of double-layered structures formed in the cytosol of uninfected macrophages. Furthermore, virus-induced four-layer forms appear to function similarly to autophagosomes and participate in the presentation of HSV-1 glycoprotein B on MHC class I. The difference in our data is that our data support a constitutively active autophagic pathway that contributes to the presentation of a self antigen by MHC class I on cancer cells.

In conclusion, the present investigation provides information on the contribution of autophagy to MHC class I processing and presentation in cancer cells but not in normal cells. Importantly, PSA displays differential susceptibilities to antigen presentation between cancer and normal cells, although it is expressed ubiquitously in both cases. Epitope creation from PSA unambiguously requires autophagic pathways, but elucidation of the more detailed molecular mechanisms and essential proteases awaits further studies. Furthermore, to what extent autophagy may participate in the generation of MHC class I-restricted epitopes remains unknown. The comprehensive analysis of peptides bound to MHC class I molecules on autophagy-knocked down cancer cells using mass spectrometry may answer the question, promoting a better understanding of cancer immunity and adding information for effective cancer immunotherapy.

Materials and Methods

Ethics Statement

The study design and purpose, after prior approval by the Institutional Review Board of the Aichi Cancer Center were fully

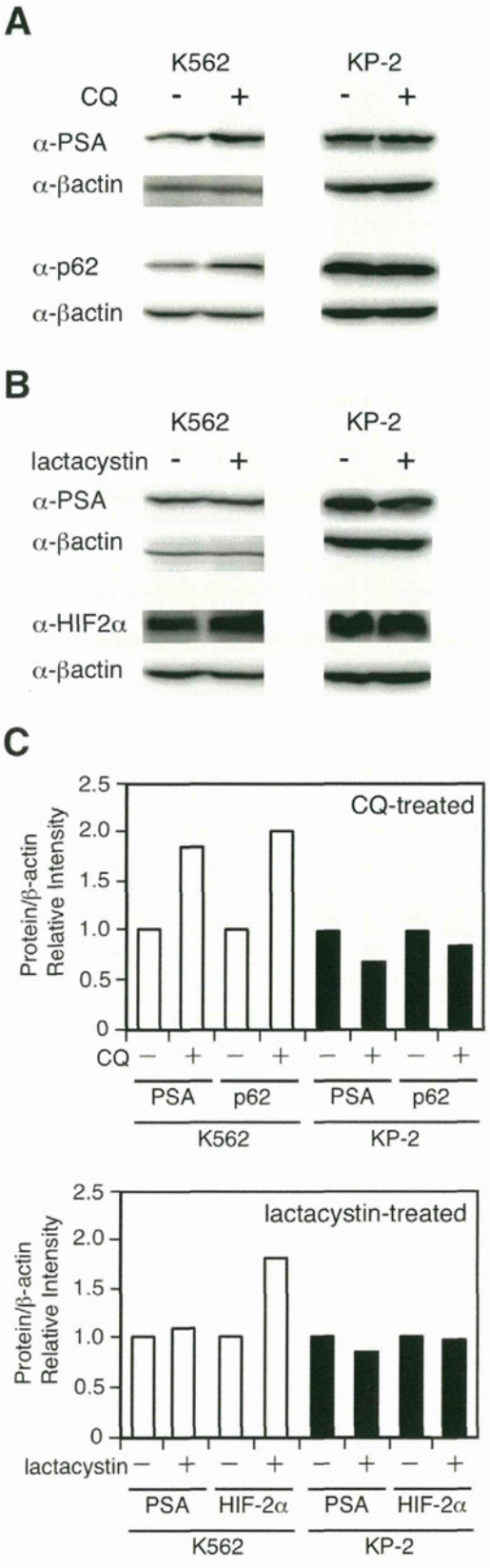

Figure 6. Degradation of full-length PSA protein is inhibited by CQ but not by lactacystin. A, Cells were cultured with or without CQ (50 μM) overnight, and then the cell lysates were subjected to Western

blot analysis for PSA and p62 as a positive control for autophagic digestion. B, Cells were cultured with or without lactacystin (5 μM) overnight, and the cell lysates were subjected to Western blot analysis for PSA and HIF-2α as a positive control for proteasomal digestion. C, The intensities of the bands were calculated using the ImageJ software.
doi:10.1371/journal.pone.0047126.g006

explained, and written consent was obtained from healthy blood donors.

Cell Lines

The human pancreatic cancer cell lines were purchased from the Japanese Collection of Research Bioresources. HLA-A24-positive normal human bronchial epithelial cells were cultured according to the supplier's recommendations (CC2540, Takara, Ohtsu, Japan). An HLA-A24-positive dermal fibroblast line and TAP-deficient T2-A24 cells were cultured as previously described [14]. The retroviral transduction of CMV 65 kDa phosphoprotein (pp65) was performed as previously described [12].

Construction of Artificial Antigen-presenting Cells (aAPCs)

Vectors carrying HLA-A*02:06, -A*24:02, mutated HLA-A*24:02, human CD86 and human 4-1BBL genes under the EF-1α promoter were constructed (CSII-EF-MCS) [41]. Lentiviral transduction was performed with similar retroviral methods [12].

CTL Induction

Naïve $CD8^+$ T cells were negatively isolated from PBMCs of A24-positive donors using the $CD8^+$ T cell isolation kit II and anti-CD45RO microbeads (Miltenyi Biotec, Bergisch Gladbach, Germany). The isolated cells were more than 95% pure $CD45RO^-$ $CD8^+$ populations. These $CD8^+$ T cells (1×10^6 cells/well) were cocultured with irradiated (100 Gy) aAPCs (1×10^5 cells/well) in 2 mL X-VIVO20 (CAMBREX, East Rutherford, NJ) supplemented with 5% human AB serum (MP Biomedicals, Solon, OH) in wells of a 12-well plate in the presence of 10 ng/mL IL-12 (Peprotech, Rocky Hill, NJ)). On day 3, 10 ng/mL IL-7 (Peprotech) and IL-15 (Peprotech) were added. Every 3 days, half the medium was exchanged for fresh medium containing 10 ng/mL IL-15. On day 12, the T cells were restimulated with γ-irradiated aAPCs. One day thereafter, IL-2 (Primmune, Kobe, Japan) was added, to a final concentration of 20 U/mL. To establish T cell clones, a limiting dilution of the polyclonal CTL was performed as previously described [14].

Detection of IFN-γ Producing $CD8^+$ T Cells

An IFN-γ secretion assay to detect IFN-γ release with a PE-labeled antibody was performed using a kit (Miltenyi Biotec) and following the manufacturer's recommendations. In inhibition assays, after an acid-stripping treatment, as described previously [42], the stimulators were incubated with drugs at the following concentrations overnight: brefeldin A (BFA, Sigma-Aldrich, St. Louis, MO), 10 μg/mL; lactacystin (Calbiochem, Darmstadt, Germany), 20 μM; chloroquine (CQ, Sigma-Aldrich), 100 μM; bafilomycin A1 (BafA, Sigma-Aldrich), 250 nM; and 3-methyladenine (3-MA, Sigma-Aldrich), 10 mM. BFA, CQ and BafA were added during co-culture with T-cells, while lactacystin and 3-MA were not. After staining, flow cytometric analysis of the stained cells was performed using a FACSCalibur (BD Biosciences, Franklin Lakes, NJ), and the data were analyzed with the help of CellQuest Pro software (BD Biosciences). Synthetic epitope peptides (Greiner, Frickenhausen, Germany) were added at concentration of 1 μg/mL to confirm intact IFN-γ production by T-cells in the presence of the drugs. In certain experiments, intracellular cytokine assessment using flow cytometry was performed instead of an IFN-γ secretion assay, as previously described [43].

Construction of a cDNA Library and Expression Screening by ELISA

The preparation of a cDNA library and expression screening were performed as described previously [44]. After overnight culture with 16F3, IFN-γ in the supernatant was measured by ELISA.

MHC Stabilization Assay

An MHC stabilization assay was performed to test the peptide for HLA-A24 binding efficiency using T2-A24 cells, as described earlier [14]. Briefly, T2-A24 cells were incubated with RPMI 1640 containing 0.1% FCS and each of the peptides at a concentration of 10 μg/mL at 26°C for 16 h, followed by incubation at 37°C for 3 h. After incubation, surface HLA-A24 molecules were stained with the anti-A24 mAb and anti-mouse FITC-conjugated Ab. HLA-A24 expression was measured using a FACSCalibur (BD Biosciences), and the mean fluorescence intensity was analyzed using the Cellquest Pro software (BD Biosciences).

IFN-γ ELISA for the Evaluation of Antigen Recognition by 16F3 with Fixed Stimulators

K562 cells expressing both HLA-A24 and CMV pp65 were fixed by various methods previously described [45,46] with slight modification as follows: fixation with 0.2% paraformaldehyde for 10 min, fixation with 0.008% glutaraldehyde for 3 min or fixation with 0.05% glutaraldehyde for 30 sec. After fixation, cells were washed with RPMI 1640 medium plus 10% FCS five times. For quenching, the cells were further washed with PBS containing 10 mM glycine two times. Following overnight co-culture of T-cell and the stimulators, the expression of IFN-γ in the cell culture supernatant was determined using an ELISA.

Plasmid Construction of HLA-A24 Mutants

A plasmid expressing HLA-A24, pcDNA3.1(+)/HLA-A24, was constructed as previously described [12]. To construct an HLA-A24-YA mutant [16] containing a single point mutation substituting an alanine residue for the tyrosine residue of exon 6, overlapping PCR [47] was performed, using pcDNA3.1(+)/HLA-A24 containing a T7 promoter primer binding site and BGH reverse priming site as a template. The following primers were used: sense primer for the T7 promoter primer-binding site, 5′-TAATACGACTCACTATAGGG-3′ (T7pp primer); internal antisense primer, 5′-CAGCCTGA-GAGGCGCTCCCTCCTTTTCTATCTGAG-3′; an internal sense primer, 5′-AAGGAGGGAGCGCCTCTCAGGCTG-CAAGCAGTGA-3′; an antisense primer for the BGH reverse priming site (BGHrp primer), 5′- TAGAAGGCACAGTC-GAGG-3′. The next PCR was performed with the first PCR products as templates, using the T7pp primer and the BGHrp primer, and produced the fusion product. To construct the HLA-A24-YA-Δ7 mutant [16] containing a complete deletion of exon 7 and a single point mutation substituting an alanine residue for the tyrosine residue of exon 6, PCR was performed with pcDNA3.1(+)/HLA-A24 as a template using the T7pp primer and an antisense primer, 5′-AAGCGGCCGCTCACACTG-CAGCCTGAGAGGCGCTCCCTCC-3′. The resultant PCR fragments were cloned into lentiviral expression vectors (CSII-

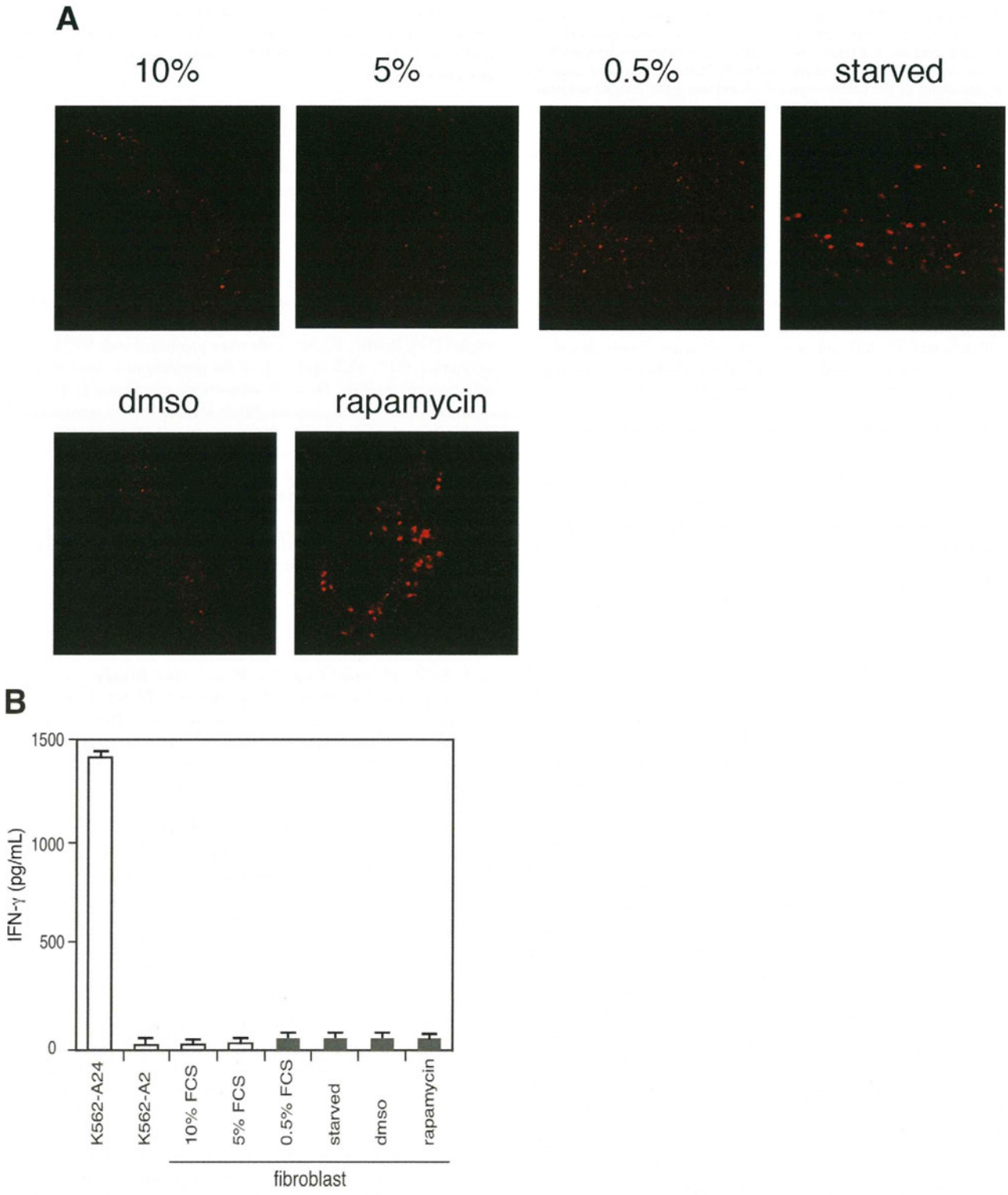

Figure 7. Induced autophagy does not result in PSA epitope presentation in fibrobast cells. A. Immunofluorescence assays for endogenous LC3 in fibroblast cells after low nutrient culture or rapamycin treatment. In low nutrient conditions, fibroblast cells were cultured in medium supplemented with 10%, 5%, 0,5% FCS or in Hank's Balanced Salt Solution (starved). B, CTL response to autophagy-induced fibroblast cells treated with low nutrient culture conditions or rapamycin. Target cells were treated with low nutrient culture conditions or rapamycin for 4h, washed twice and cultured with CTL overnight. Next day, supernatants were harvested and IFN-γ measured by ELISA. K562-A24 cells and K562-A2 cells were used as positive and negative control, respectively. The results show means ± SD of triplicates.
doi:10.1371/journal.pone.0047126.g007

EF-MCS). The cloned genes were sequenced to verify their identity.

Immunofluorescence Microscopy

Cells on glass coverslips were fixed for 10 min with PBS containing 3% paraformaldehyde. After washing, the cells were permeabilized with 50 μg/mL digitonin (Sigma-Aldrich) in PBS for 5 min at room temperature. The cells were then washed and blocked with 3% BSA in PBS for 10 min. After probing with a rabbit Ab specific to human PSA (GeneTex, Irvine, CA) and a mouse mAb specific to human LC3 (4E12, MBL, Nagoya, Japan) for 1 h, secondary Abs conjugated to Alexa 488 and 594 (Invitrogen, Carlsbad, CA) were applied for 30 min. All of the immunochemical assays were performed at room temperature. The slides were mounted in ProLong Gold antifade reagent (Invitrogen). Confocal fluorescence images were obtained using a confocal laser-scanning microscope (LSM510 META; Carl Zeiss, Göttingen, Germany) with a Plan-Apochromat 63x/1.40- or 100x/1.40- numerical -aperture oil immersion lens and LSM Image Browser software (Carl Zeiss).

Western Blot Analysis

Western blot analysis was performed as described previously [48]. A mouse mAb specific to human PSA (#2649C4a; Cosmo Bio, Tokyo, Japan), p62 (5F2; MBL) HIF2α (#NB100-132; NOVUS, Littleton, CO) or β-actin (Sigma-Aldrich), or a rabbit Ab specific to human LC3 (MBL) was used. All of the images were processed by Lumi Vision Pro 400EX (Aisin/Taitec, Inc., Kariya, Japan). The signal intensity was quantified with the ImageJ software.

Transfection with Small Interfering RNAs (siRNAs)

SiRNAs specific for PSA, autophagy-related gene (atg)5 and atg7 were created using Stealth™ RNAi preparations and obtained from Invitrogen. The target sequences are as follows: PSA-siRNA-1, GGAGGAUUCUUAAUAUCCAGACUAA; PSA-siRNA-2, CAGCUCUGCCAUGCUGGAAAGUUUA; PSA-siNRA-3, CCAAACCUGGAGAAGGUCAUCUCGA; atg5-siRNA-1, UCGAGAUGUGUGGUUUGGACGAAUU; atg5-siRNA-2, AAGCAACUCUGGAUGGGAUUGCAAA; atg5-siRNA-3, CCUCAAAGAAGUUUGUCCUUCUGCU; atg7-siRNA-1, CAGAAGGAGUCACAGCUCUUCCUUA; atg7-siRNA-2, GAAAGCCAUGAUGUCGUCUUCCUAU; and atg7-siRNA-3, GGCCGUGGAAUUGAUGGUAUCUGUU. A scrambled siRNA (Invitrogen) was used for negative control. The KP-3 and MIA PaCa-2 cells (2×10^5 cells/well) were transfected with each siRNA (100 nM) using Lipofectamine 2000 (Invitrogen) in 24-well plates. After 70 h, the cells were harvested and used in an ELISA, or the total RNA was extracted using the RNAeasy mini kit (Qiagen, Tokyo, Japan) with DNase I treatment, and reverse transcription was performed in 20-ul reactions containing oligo $(dT)_{20}$ primers and 0.5 μg aliquots. The alignments of specific primer sets were as follows: PSA and PSA variant common forward, 5′-TCCATCTGAGGTTGATGAGAT-3′; PSA reverse, 5′-TCCACATAAATGAGGGGAAATC-3′; PSA variant reverse, 5′-GTCCCAGCCTGGATAGAGTG-3′; atg5 forward, 5′-TGGGATTGCAAAATGACAGA-3′; atg5 reverse, 5′-CACTGCAGAGGTGTTTCCAA-3′; atg7 forward, 5′-GAAACCAAAGCAGCAAGGAG-3′; and atg7 reverse, 5′-CATTCATCCGATCGTCACTG-3′. The PCR products were separated in 2.0% agarose and visualized with ethidium bromide staining.

Supporting Information

Figure S1 Identification of PSA variant cDNA encoding an epitope recognized by 16F3. A, HLA-A24-expressing HEK293T (A24-293T) cells were transfected with each plasmid from a cDNA library constructed from mRNA extracted K562 cells. IFN-γ was measured by ELISA. Arrow indicates a well of 8G containing an antigenic plasmid. B, The cDNA clone was a variant PSA (NM_006310). The schematic drawing of full length (top) and variant (bottom) PSA is shown. The variant is an intronic polyadenylated mRNA ending with the exon 12 and a following intron. C-D, Identification of an epitope peptide recognized by 16F3. A24-293T cells were transfected with each plasmid encoding truncated fragments. The constructs shown as open boxes were recognized by 16F3, while that shown as filled boxes were not. Numbers indicate amino acid positions (C). Minigenes were cloned into pcDNA3.1(+) plasmid and transfected into A24-293T cells. The amino acid sequences were shown in one-letter code, and defined epitope is underlined (D). E, MHC stabilization assay was executed without peptide or with either synthetic 12mer peptide, DYFNVPYPLPKI or control CMV peptide, QYDP-VAALF. F, T2-A24 cells were pulsed with serial concentrations of either synthetic 12mer peptide, DYFNVPYPLPKI (diamond) or control CMV peptide, QYDPVAALF (circle). Release of IFN-γ was measured by ELISA. The results are the mean of triplicate values.
(TIF)

Figure S2 Peptide-pulsed KP-2 and SUIT-2 cells were recognized by 16F3. KP-3 (white), KP-2 (black) and SUIT-2 (vertical stripe) cells were pulsed with either synthetic 12mer peptide, DYFNVPYPLPKI (DYF) or control CMV peptide, QYDPVAALF (QYD) ate a concentration of 1 μM. Release of IFN-γ was measured by ELISA.
(TIF)

Figure S3 Fixation of target cells abolish recognition by 16F3, which is not recovered by glycine quenching. A–B, K562 cells transfected with CMV pp65 and HLA-A24 were used as stimulators for either 16F3 or an HLA-A24-restricted CMV pp65-specific CTL clone. A, Stimulators were fixed in three ways; 0.2% paraformaldehyde (PFA) for 10 min, 0.008% glutaraldehyde (GA) for 3 min, or 0.05% glutaraldehyde (GA) for 30 sec. After fixation, cells were washed 5 times with RPMI medium containing 10% FCS. B, Fixed and washed stimulators were further washed two times with PBS containing 10 mM glycine for quenching. The stimulators were cultured with each clone and IFN-γ in the supernatants was measured by ELISA. The data express mead of duplicates.
(TIF)

Figure S4 The epitope is not presented by recycling HLA-A24 molecules. A, The amino acid sequences of the cytoplasmic portion of the wild-type HLA-A24 (WT-A24) and two endosome recycling-compromised mutants, designated as A24-YA and A24-YAΔ7, are shown as a single letter code. S, signal sequence; TM, transmembrane domain; CY, cytoplasmic domain. B, Surface expression of HLA-A24 or its mutant molecules on lentiviral-transfected K562 cells was measured using a flow cytometer. C, K562 cells transfected with CMV pp65 accompanied by HLA-A02, HLA-A24 or its mutant were incubated with either 16F3 or an HLA-A24-restricted CMV pp65-specific CTL clone, and an IFN-γ ELISA was performed. The results are expressed as the means of triplicate experiments.
(TIF)

Figure S5 Surface HLA expression of HLA-A24-expressing K562 cells treated with acid buffer and 3-methyladenine (3-MA). The surface expression of the HLA class I molecule of HLA-A24-expressing K562 cells was examined with a flow cytometer after the cells were treated with acid buffer for peptide stripping and incubated with or without 3-MA for 14 h. The white and shaded areas show samples incubated with FITC-labeled anti-HLA class I and isotype control mAb, respectively. Stained cells were analyzed using a flow cytometer.
(TIF)

Figure S6 The surface HLA expression of siRNA-transfected pancreatic carcinoma cells. KP-3 (A) and MIA PaCa-2 (B) cells were transfected with scrambled, atg5, or atg7-specific siRNA for 70 h. The white and shaded areas show samples incubated with FITC-labeled anti-HLA class I and isotype control mAb, respectively. The stained cells were analyzed using a flow cytometer.
(TIF)

Acknowledgments

The authors of this paper thank Dr. M. Fujita for critically reading the manuscript, Dr. R. Ohta, Dr. M. Ibi and Dr. Y. Shibata-Watanabe for their technical expertise, and Ms. H. Tamaki for her secretarial assistance.

Author Contributions

Conceived and designed the experiments: ADO KK. Performed the experiments: ADO. Analyzed the data: ADO KK. Contributed reagents/materials/analysis tools: HT YA HM TY. Wrote the paper: ADO KK.

References

1. York IA, Rock KL (1996) Antigen processing and presentation by the class I major histocompatibility complex. Annu Rev Immunol 14: 369–396.
2. Klionsky DJ, Emr SD (2000) Autophagy as a regulated pathway of cellular degradation. Science 290: 1717–1721.
3. Mathew R, Karantza-Wadsworth V, White E (2007) Role of autophagy in cancer. Nat Rev Cancer 7: 961–967.
4. Deretic V (2005) Autophagy in innate and adaptive immunity. Trends Immunol 26: 523–528.
5. Levine B, Deretic V (2007) Unveiling the roles of autophagy in innate and adaptive immunity. Nat Rev Immunol 7: 767–777.
6. Nimmerjahn F, Milosevic S, Behrends U, Jaffee EM, Pardoll DM, et al. (2003) Major histocompatibility complex class II-restricted presentation of a cytosolic antigen by autophagy. Eur J Immunol 33: 1250–1259.
7. Paludan C, Schmid D, Landthaler M, Vockerodt M, Kube D, et al. (2005) Endogenous MHC class II processing of a viral nuclear antigen after autophagy. Science 307: 593–596.
8. Butler MO, Lee JS, Ansen S, Neuberg D, Hodi FS, et al. (2007) Long-lived antitumor CD8+ lymphocytes for adoptive therapy generated using an artificial antigen-presenting cell. Clin Cancer Res 13: 1857–1867.
9. Tian B, Pan Z, Lee JY (2007) Widespread mRNA polyadenylation events in introns indicate dynamic interplay between polyadenylation and splicing. Genome Res 17: 156–165.
10. Kubo RT, Sette A, Grey HM, Appella E, Sakaguchi K, et al. (1994) Definition of specific peptide motifs for four major HLA-A alleles. Journal of immunology 152: 3913–3924.
11. Constam DB, Tobler AR, Rensing-Ehl A, Kemler I, Hersh LB, et al. (1995) Puromycin-sensitive aminopeptidase. Sequence analysis, expression, and functional characterization. J Biol Chem 270: 26931–26939.
12. Kondo E, Akatsuka Y, Kuzushima K, Tsujimura K, Asakura S, et al. (2004) Identification of novel CTL epitopes of CMV-pp65 presented by a variety of HLA alleles. Blood 103: 630–638.
13. English L, Chemali M, Duron J, Rondeau C, Laplante A, et al. (2009) Autophagy enhances the presentation of endogenous viral antigens on MHC class I molecules during HSV-1 infection. Nat Immunol 10: 480–487.
14. Kuzushima K, Hayashi N, Kimura H, Tsurumi T (2001) Efficient identification of HLA-A*2402-restricted cytomegalovirus-specific CD8(+) T-cell epitopes by a computer algorithm and an enzyme-linked immunospot assay. Blood 98: 1872–1881.
15. Gromme M, Uytdehaag FG, Janssen H, Calafat J, van Binnendijk RS, et al. (1999) Recycling MHC class I molecules and endosomal peptide loading. Proc Natl Acad Sci U S A 96: 10326–10331.
16. Lizee G, Basha G, Tiong J, Julien JP, Tian M, et al. (2003) Control of dendritic cell cross-presentation by the major histocompatibility complex class I cytoplasmic domain. Nat Immunol 4: 1065–1073.
17. Vega MA, Strominger JL (1989) Constitutive endocytosis of HLA class I antigens requires a specific portion of the intracytoplasmic tail that shares structural features with other endocytosed molecules. Proc Natl Acad Sci U S A 86: 2688–2692.
18. Lizee G, Basha G, Jefferies WA (2005) Tails of wonder: endocytic-sorting motifs key for exogenous antigen presentation. Trends Immunol 26: 141–149.
19. van Weert AW, Geuze HJ, Groothuis B, Stoorvogel W (2000) Primaquine interferes with membrane recycling from endosomes to the plasma membrane through a direct interaction with endosomes which does not involve neutralisation of endosomal pH nor osmotic swelling of endosomes. Eur J Cell Biol 79: 394–399.
20. Kimura S, Noda T, Yoshimori T (2007) Dissection of the autophagosome maturation process by a novel reporter protein, tandem fluorescent-tagged LC3. Autophagy 3: 452–460.
21. Mizushima N, Yoshimori T, Levine B (2010) Methods in mammalian autophagy research. Cell 140: 313–326.
22. Schmid D, Munz C (2007) Innate and adaptive immunity through autophagy. Immunity 27: 11–21.
23. Klionsky DJ (2005) The molecular machinery of autophagy: unanswered questions. J Cell Sci 118: 7–18.
24. Komatsu M, Waguri S, Koike M, Sou YS, Ueno T, et al. (2007) Homeostatic levels of p62 control cytoplasmic inclusion body formation in autophagy-deficient mice. Cell 131: 1149–1163.
25. Chen L, Uchida K, Endler A, Shibasaki F (2007) Mammalian tumor suppressor Int6 specifically targets hypoxia inducible factor 2 alpha for degradation by hypoxia- and pVHL-independent regulation. J Biol Chem 282: 12707–12716.
26. Nagata Y, Hanagiri T, Takenoyama M, Fukuyama T, Mizukami M, et al. (2005) Identification of the HLA-Cw*0702-restricted tumor-associated antigen recognized by a CTL clone from a lung cancer patient. Clin Cancer Res 11: 5265–5272.
27. Robbins PF, el-Gamil M, Li YF, Topalian SL, Rivoltini L, et al. (1995) Cloning of a new gene encoding an antigen recognized by melanoma-specific HLA-A24-restricted tumor-infiltrating lymphocytes. J Immunol 154: 5944–5950.
28. Ogier-Denis E, Houri JJ, Bauvy C, Codogno P (1996) Guanine nucleotide exchange on heterotrimeric Gi3 protein controls autophagic sequestration in HT-29 cells. J Biol Chem 271: 28593–28600.
29. Liang XH, Yu J, Brown K, Levine B (2001) Beclin 1 contains a leucine-rich nuclear export signal that is required for its autophagy and tumor suppressor function. Cancer Res 61: 3443–3449.
30. Proikas-Cezanne T, Waddell S, Gaugel A, Frickey T, Lupas A, et al. (2004) WIPI-1alpha (WIPI49), a member of the novel 7-bladed WIPI protein family, is aberrantly expressed in human cancer and is linked to starvation-induced autophagy. Oncogene 23: 9314–9325.
31. Susan PP, Dunn WA, Jr. (2001) Starvation-induced lysosomal degradation of aldolase B requires glutamine 111 in a signal sequence for chaperone-mediated transport. J Cell Physiol 187: 48–58.
32. Ito H, Daido S, Kanzawa T, Kondo S, Kondo Y (2005) Radiation-induced autophagy is associated with LC3 and its inhibition sensitizes malignant glioma cells. Int J Oncol 26: 1401–1410.
33. Fujii S, Mitsunaga S, Yamazaki M, Hasebe T, Ishii G, et al. (2008) Autophagy is activated in pancreatic cancer cells and correlates with poor patient outcome. Cancer Sci 99: 1813–1819.
34. Yang S, Wang X, Contino G, Liesa M, Sahin E, et al. (2011) Pancreatic cancers require autophagy for tumor growth. Genes Dev 25: 717–729.
35. Guo JY, Chen HY, Mathew R, Fan J, Strohecker AM, et al. (2011) Activated Ras requires autophagy to maintain oxidative metabolism and tumorigenesis. Genes Dev 25: 460–470.
36. Kim MJ, Woo SJ, Yoon CH, Lee JS, An S, et al. (2011) Involvement of autophagy in oncogenic K-Ras-induced malignant cell transformation. J Biol Chem 286: 12924–12932.
37. Iguchi H, Morita R, Yasuda D, Takayanagi R, Ikeda Y, et al. (1994) Alterations of the p53 tumor-suppressor gene and ki-ras oncogene in human pancreatic cancer-derived cell-lines with different metastatic potential. Oncol Rep 1: 1223–1227.
38. Burrows SR, Rossjohn J, McCluskey J (2006) Have we cut ourselves too short in mapping CTL epitopes? Trends Immunol 27: 11–16.
39. Ebert LM, Liu YC, Clements CS, Robson NC, Jackson HM, et al. (2009) A long, naturally presented immunodominant epitope from NY-ESO-1 tumor antigen: implications for cancer vaccine design. Cancer Res 69: 1046–1054.
40. Tynan FE, Burrows SR, Buckle AM, Clements CS, Borg NA, et al. (2005) T cell receptor recognition of a 'super-bulged' major histocompatibility complex class I-bound peptide. Nat Immunol 6: 1114–1122.
41. Miyoshi H, Blomer U, Takahashi M, Gage FH, Verma IM (1998) Development of a self-inactivating lentivirus vector. J Virol 72: 8150–8157.

42. Sugawara S, Abo T, Kumagai K (1987) A simple method to eliminate the antigenicity of surface class I MHC molecules from the membrane of viable cells by acid treatment at pH 3. J Immunol Methods 100: 83–90.
43. Kuzushima K, Hoshino Y, Fujii K, Yokoyama N, Fujita M, et al. (1999) Rapid determination of Epstein-Barr virus-specific CD8(+) T-cell frequencies by flow cytometry. Blood 94: 3094–3100.
44. Torikai H, Akatsuka Y, Miyazaki M, Tsujimura A, Yatabe Y, et al. (2006) The human cathepsin H gene encodes two novel minor histocompatibility antigen epitopes restricted by HLA-A*3101 and -A*3303. Br J Haematol 134: 406–416.
45. Burdin N, Brossay L, Koezuka Y, Smiley ST, Grusby MJ, et al. (1998) Selective ability of mouse CD1 to present glycolipids: alpha-galactosylceramide specifically stimulates V alpha 14+ NK T lymphocytes. J Immunol 161: 3271–3281.
46. Burgdorf S, Scholz C, Kautz A, Tampe R, Kurts C (2008) Spatial and mechanistic separation of cross-presentation and endogenous antigen presentation. Nat Immunol 9: 558–566.
47. Ho SN, Hunt HD, Horton RM, Pullen JK, Pease LR (1989) Site-directed mutagenesis by overlap extension using the polymerase chain reaction. Gene 77: 51–59.
48. Tajima K, Demachi A, Ito Y, Nishida K, Akatsuka Y, et al. (2004) Identification of an epitope from the epithelial cell adhesion molecule eliciting HLA-A*2402-restricted cytotoxic T-lymphocyte responses. Tissue Antigens 64: 650–659.

Chimerism 1:1, 39-43; July/August/September 2010; © 2010 Landes Bioscience

Long-term feto-maternal microchimerism revisited

Microchimerism and tolerance in hematopoietic stem cell transplantation

Tatsuo Ichinohe

Department of Hematology and Oncology; Graduate School of Medicine; Kyoto University; Kyoto, Japan

Key words: fetal microchimerism, maternal microchimerism, hematopoietic stem cell transplantation, graft-versus-host disease, acquired tolerance, non-inherited maternal antigens, inherited paternal antigens, T regulatory cells, trans-vivo delayed-type hypersensitivity assay

Abbreviations: DTH, delayed-type hypersensitivity; GVHD, graft-versus-host disease; HSC, hematopoietic stem cell; IPA, inherited paternal antigen; mHAg, minor histocompatibility antigen; NIMA, noninherited maternal antigen; PBMC, peripheral blood mononuclear cell; TGF, transforming growth factor; T_E cells, T effector cells; T_R cells, T regulatory cells

Submitted: 06/09/10

Accepted: 06/21/10

Previously published online: http://www.landesbioscience.com/journals/chimerism/article/12743

DOI: 10.4161/chim.1.1.12743

Correspondence to: Tatsuo Ichinohe; Email: nohe@kuhp.kyoto-u.ac.jp

Bidirectional fetal-maternal cell traffic during pregnancy gives rise to stable persistence of minute amounts of allogeneic cells both in the mother and in her offspring, a phenomenon called long-term fetal or maternal microchimerism. Over the past decade, increasing attention has been devoted to elucidating the biological relevance of such reciprocal microchimerism, unveiling its conflicting roles in either immune sensitization or tolerance induction against fetal or maternal alloantigens. Recent studies in mice and humans have highlighted the significance of fetal-maternal microchimerism in the induction and maintenance of $CD4^+CD25^+$ and $CD8^+$ T regulatory cells that counterbalance the immune responses to fetal or maternal antigens mediated by T effector cells. Consistent with these observations, T-cell-replete hematopoietic stem cell transplantation between mutually microchimeric mothers and their HLA-haploidentical offspring has been shown to be feasible, although the degree of microchimerism-associated tolerance appears to substantially differ among the cases. Since in vitro or trans-vivo assays to detect antigen-specific tolerance in the context of the T regulator versus T effector balance are now available, future clinical studies incorporating these tests into the criteria for donor selection are warranted to more precisely define the relevance of fetal-maternal microchimerism in allotolerance and immune homeostasis after hematopoietic stem cell transplantation.

Introduction

Long-lasting bidirectional tolerance between the donor and recipient without excessive pharmacologic immunosuppression has been one of the ultimate but unfeasible goals in allogeneic hematopoietic stem cell (HSC) transplantation. Especially in the setting of HSC transplants from genetically HLA-disparate donors, substantial proportions of patients receiving intensive immunosuppressive agents still suffer from graft rejection or severe graft-versus-host disease (GVHD), either of which significantly compromises post-transplant survival outcomes. Given the ever-increasing number of HSC transplants with the use of donors other than HLA-identical siblings, it is crucially important to further elucidate the immunologic mechanisms by which HLA-incompatible HSC allografts are successfully accepted by some recipients but not by others.

Fetal-maternal microchimerism is a form of naturally acquired microchimerism that commonly occurs among eutherian mammals through two-way nucleated cell exchanges between the mother and fetus during the course of normal pregnancy.[1-3] With the help of flow cytometric cell sorting and highly sensitive polymerase chain reactions, minute amounts of hematopoietic cells and/or DNA of fetal origin can be detected in the blood and tissues of the respective mothers as long as decades postpartum,[4,5] while low levels of maternal cells can be identified not only in the various tissues of the fetus but in the peripheral circulation of the

immunocompetent adult offspring.[6,7] Thus far the biological relevance of such long-term persistent microchimerism is not fully characterized, although earlier observations suggested its possible roles in immune sensitization against fetal or maternal alloantigens.[1-3] Long-term fetal microchimerism in parous women has been reported to be associated with susceptibility to a variety of autoimmune disorders and protection from certain cancers.[1,2,8,9] Similarly, persistence of maternal microchimerism in immunocompetent offspring was suggested to be involved in the pathogenic mechanisms underlying immune-mediated pediatric diseases such as neonatal lupus syndrome and biliary atresia.[10,11]

In addition to functioning as sources for alloantigens to prime immune effectors, fetal-maternal microchimerism is now emerging as a crucial player involved in the induction and maintenance of pregnancy-associated immune tolerance toward fetal inherited paternal antigens (IPAs) in mothers as well as toward noninherited maternal antigens (NIMAs) in their progeny.[12] In the past several years, the feasibility of HSC transplants from HLA-haploidentical microchimeric donors has been explored to improve donor availability and transplant outcomes based on the hypothesis that maternal donors with fetal microchimerism are rendered immunologically hyporesponsive to their offspring and vice versa, offspring donors harboring maternal microchimerism are rendered tolerant to both their mothers and HLA-haploidentical siblings expressing NIMAs as mismatched histocompatibility antigens. In this brief article, we will discuss the promises and challenges of such HSC transplants from donors with fetal or maternal microchimerism in the light of future directions to take more advantage of microchimerism-associated immune equilibrium by employing assays to evaluate and means to enhance the robustness of IPA- or NIMA-specific tolerance probably determined by balance between T regulator and T effector cells responsive to fetal or maternal alloantigens.

Clinical and Experimental Observations Linking Long-Term Fetal-Maternal Microchimerism to Hematopoietic Cell Allograft Tolerance

A possible linkage between fetal microchimerism and HSC allograft tolerance was initially suggested by Tokita et al. who reported a case of a woman with refractory thymic carcinoma successfully treated with an infusion of allogeneic peripheral blood stem cells from her HLA-haploidentical daughter.[13] This woman was revealed to harbor microchimerism presumed to have originated from the daughter prior to and 11 months after the stem cell infusion. It was speculated that the infused donor cells could survive in face of the maternal immune system probably because the recipient mother had already become rendered hyporesponsive to IPAs of her daughter. Furthermore, the mother had no clinical manifestations of GVHD throughout the treatment period, implyng the presence of reciprocal tolerance to NIMAs in the daughter. Soon thereafter, Ochiai et al. reported a case of a young male patient with refractory leukemia who underwent successful non-T-cell-depleted peripheral blood stem cell transplantation from his microchimeric mother, setting the first milestone for the clinical development of HSC donor selection based on fetal-maternal microchimerism.[14] Notably, it was recently reported that HLA-haploidentical lymphocyte infusions from mothers harboring long-term fetal microchimerism were also effective in eradicating Epstein-Barr virus-positive T-cell lymphoproliferative diseases developed in their offspring without causing obvious GVHD.[15]

A close association of maternal microchimerism with acquisition and maintenance of specific tolerance to NIMAs has been more clearly demonstrated through a series of studies in mice and humans.[16-18] With the use of the murine F_1 x P backcross breeding model (B6 x BDF1) to generate H-$2^{b/b}$ offspring mice exposed to H-2^{d} as NIMA in utero and/or via breastfeeding, Zhang and Miller for the first time demonstrated that NIMA-exposed mice showed prolonged acceptance of maternal skin allografts while the period of graft survival was positively correlated with the amount of naturally transferred maternal T cells in their lymph nodes.[16] Andrassy and Kusaka et al. employed the same murine model and showed that NIMA-exposed offspring achieving tolerance to fully allogeneic H-$2^{d/d}$ heart allografts had relatively higher levels of maternal microchimerism in the lymphoid organs.[17] Importantly, human fetal lymphid organs also contain microchimeric maternal cells,[7,18] and subsequent experiments in mice and humans revealed that the tolerogenic NIMA effects were dependent on $CD4^+CD25^+$ T cells capable of suppressing alloreactive T-cell responses to maternal antigens.[18,19] These observations strongly suggested the crucial role of microchimeric maternal cells to generate NIMA-specific $CD4^+CD25^{high}Foxp3^+$ T regulatory cells in the offspring. It is also an intriguing and important question whether a similar mechanism can operate in parous women harboring fetal microchimerism because $CD4^+CD25^+$ T regulatory cells were also demonstrated to be involved in the induction and maintenance of maternal tolerance to the fetus in a murine model.[20]

Clinical Results of HLA-haploidentical Hematopoietic Stem Cell Transplantation from Donors Harboring Fetal or Maternal Microchimerism

In support of the above-mentioned observations, it has been reported that HSC transplants from mothers or NIMA-mismatched siblings confer superior outcomes as compared to those from fathers or siblings without NIMA mismatch as HSC donors,[21-23] probably suggesting better posttransplant immune reconstitution in the presence of IPA or NIMA mismatch. To further extend the availability of HLA-incompatible donors with the help of remote influence of fetal-maternal tolerance, we have explored the feasibility of T-cell-replete HSC transplantation from HLA-haploidentical family donors harboring persistent fetal or maternal microchimerism in the peripheral circulation.[24] These transplants involved three different types of donor-recipient combination: (i) transplantation from mothers

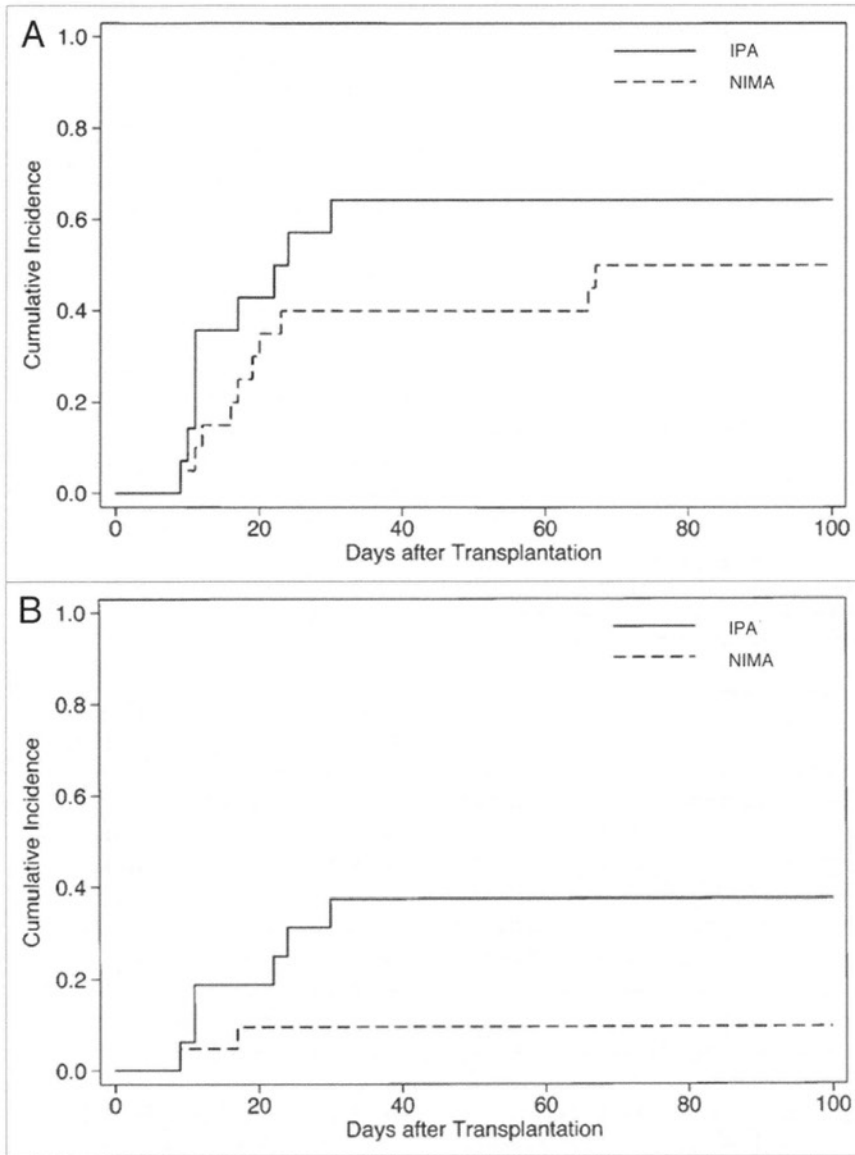

Figure 1. Cumulative incidence of acute GVHD in patients who underwent hematopoietic cell transplantation from an HLA-haploidentical related donor harboring fetal or maternal microchimerism. Cumulative incidence of moderate-to-severe (grade 2–4) (A) and severe (grade 3 or 4) (B) acute GVHD according to the type of HLA mismatch among 34 evaluable patients who received T-cell-replete HSC transplantation from an HLA-haploidentical related donor harboring fetal or maternal microchimerism. Solid line, transplants from mothers to their offspring (IPA mismatch in the GVH vector); dashed line, transplants from offspring to their mothers or to NIMA-mismatched siblings (NIMA mismatch in the GVH vector). This research was originally published in Blood.[24] Ichinohe T, et al. Feasibility of HLA-haploidentical hematopoietic stem cell transplantation between noninherited maternal antigen (NIMA)-mismatched family members linked with long-term feto-maternal microchimerism. Blood 2004; 104:3821–8. © The American Society of Hematology.

carrying microchimerism of fetal origin to their respective offspring, a setting that microchimerism-associated allotolerance in the donor might favorably modulate GVH responses against IPAs; (ii) transplantation from offspring carrying maternal microchimerism to their mothers or (iii) to their NIMA-mismatched HLA-haploidentical siblings, a setting that microchimerism-associated allotolerance in the donor might ameliorate GVH responses against NIMAs.[3]

Based on this scheme, we analyzed clinical outcomes of 35 patients with high-risk hematologic malignancy who received T-cell-replete HSC allografts from donors with fetal or maternal microchimerism.[24] With the use of conventional tacrolimus-based GVHD prophylaxis, all patients achieved durable engraftment and 19 (56%) of 34 evaluable patients developed grade 2–4 acute GVHD (**Fig. 1A**). In this study, the presence of NIMA mismatch in the GVH direction was associated with lower risk of developing severe acute GVHD as compared with IPA mismatch (**Fig. 1B**), although this observation should be reevaluated in a larger prospective cohort. Recently, we have updated information regarding survival of these patients and confirmed that such transplants conferred acceptable probabilities of long-term disease-free survival (**Fig. 2**). A series of case reports have also shown the feasibility of HLA-mismatched HSC donor selection based on fetal-maternal microchimerism,[12] but some cases are still associated with graft rejection and severe acute GVHD.[25] Furthermore, longer follow-up of these patients lead to a paradoxical observation that substantial proportions of survivors could discontinue administration of immunosuppressive agents despite the frequent occurrence of chronic GVHD requiring systemic treatment,[26] raising a new question as to the role of fetal-maternal microchimerism as an indicator of clinically relevant tolerance toward IPAs or NIMAs.

Equilibrium between T Regulatory Cells and T Effector Cells as a Mechanism to Determine the Net Immune Responses against Fetal or Maternal Alloantigens

Apparently conflicting results with respect to HSC transplants from microchimeric donors can be clearly reconciled by recent studies demonstrating that the tolerance associated with long-term fetal-maternal microchimerism would be determined by the balance between T regulatory cells (T_R) and T effector (T_E) cells specific for IPAs or NIMAs.[27-29] Cai et al. explored the role of minor histocompatibility antigen (mHAg) HA-1 in the allograft tolerance of three patients who received kidney transplants from an HLA-matched but HA-1-mismatched family member.[27] By

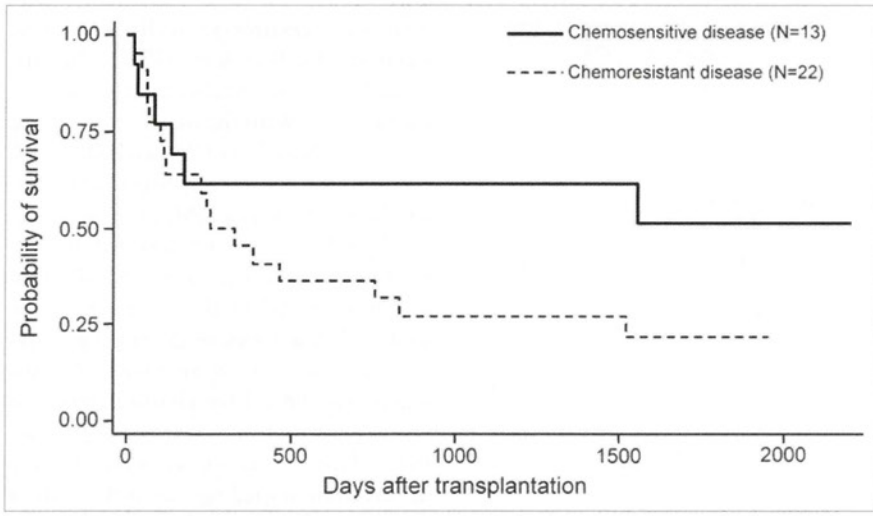

Figure 2. Long-term survival of patients who underwent hematopoietic cell transplantation from an HLA-haploidentical related donor harboring fetal or maternal microchimerism. Kaplan-Meier estimates of overall survival with a median follow-up of 4.6 years in 35 patients who received T-cell-replete HSC transplantation from an HLA-haploidentical related donor harboring fetal or maternal microchimerism for advanced hematologic malignancies. Solid line, transplants in remission; dashed line, transplants in chemotherapy-refractory disease.

analyzing peripheral blood mononuclear cells (PBMCs) obtained from these recipients with the use of HA-1-specific tetramer staining, they were able to detect two distinct tetramer-positive $CD8^+$ T-cell populations: the tetramer brightly positive population with characteristics of T_E cells that produces IFNγ and the tetramer dimly positive population with characteristics of T_R cells that produces IL-10 and transforming growth factor (TGF)β. Trans-vivo injection of PBMCs of these three patients into the footpads of severe combined immunodeficiency mice lead to IL-10 and/or TGFβ-regulated delayed-type hypersensitivity (DTH) responses to HA-1 peptide. The suppression of these T_E cell functions by HA-1 tetramer dimly positive $CD8^+$ T_R cells was dependent on IL-10, TGFβ and cytotoxic T lymphocyte-associated antigen 4 (CTLA-4). Intriguingly, these recipients were proven to harbor microchimerism of HA-1-positive dendritic cells. This report was the first demonstration of coexistence of microchimeric cells carrying mHAg, T_E cells responding to mHAg and T_R cells that are capable of suppressing mHAg-specific T_E cell functions, thus suggesting an essential role of microchimeric cells as a reservoir of alloantigens that are required for maintenance of both mHAg-specific T_E and T_R cells.

Recently, van Halteren et al. provided more robust evidence that parous women and their healthy offspring can persistently harbor mHAg-specific $CD8^+$ T_R cells bearing low-avidity T-cell receptors as well as $CD8^+$ cytotoxic T cells reactive to the same mHAg. With the use of PBMCs of healthy mother-offspring pairs mismatched for HY and/or HA-1 antigens, the presence of mHAg-specific $CD8^+$ T_R cells was analyzed in the trans-vivo DTH assays and a substantial proportion of mothers and offspring were found to harbor mHAg tetramer-dimly positive T_R cells functioning in a CTLA-4-dependent manner. Importantly, they also showed that the functional balance between T_R cells versus T_E cells significantly differ among individuals, providing a clue to explain the differential immunogenicity against IPAs or NIMAs observed in the setting of clinical HSC transplantation.

In a subsequent study using a murine model, Dutta et al. showed that the levels and tissue distribution of maternal microchimerism are strongly correlated with maintenance of NIMA-specific T_R cells in mice developmentally and neonatally exposed to NIMA.[29] Levels of maternal microchimerism were positively correlated with NIMA-specific suppression of both DTH and in vivo mixed lymphoproliferative reactions. Remarkably, when mice were exposed to NIMA only in utero and lacked oral exposure to NIMA via breastfeeding, maternal microchimerism was lost in association with emergence of sensitized DTH responses against NIMA. Collectively, these findings support the scenario that modes of immune responses toward IPAs in parous females as well as those toward NIMAs in offspring are determined by the positive or negative net balance between IPA- or NIMA-specific T_R cells and T_E cells, which might be correlated with levels of persistent fetal or maternal microchimerism and specific donor-recipient combinations of histocompatibility antigens.[30]

Future Directions and Conclusions

Accumulating lines of evidence from mice and humans have indicated the close association between long-term fetal-maternal microchimerism and the development of IPA- or NIMA-specific $CD4^+CD25^+$ and $CD8^+$ T_R cells. Since the immune equilibrium in favor of T_R cells versus T_E cells appears to be necessary for the maintenance of IPA- or NIMA-specific tolerance, future studies to improve the outcome of HSC transplants should aim at identifying means to enhance such tolerance in HSC donors harboring long-term fetal or maternal microchimerism. Because breastfeeding appears to be an indispensable mechanism to establish robust NIMA-specific tolerance, it is intriguing to investigate whether oral administration of NIMA peptide can promote the generation of NIMA-specific T_R cells in adult offspring previously exposed to NIMAs. In a similar fashion, whether oral or non-oral exposure to IPAs may affect IPA-specific immune responses in mothers harboring fetal microchimerism remains an open question. Since laboratory tests to evaluate T_R versus T_E balance such as allopeptide-specific tetramer staining or trans-vivo DTH assays have now become available, further clinical studies incorporating these tests into the criteria for microchimeric HSC donor selection are warranted to clarify the relevance of fetal-maternal microchimerism in establishing allospecific tolerance after hematopoietic stem cell transplantation.

References

1. Adams KM, Nelson JL. Microchimerism: an investigative frontiers in autoimmunity and transplantation. JAMA 2004; 291:1127-31.
2. Klonisch T, Drouin R. Fetal-maternal exchange of multipotent stem/progenitor cells: microchimerism in diagnosis and disease. Trends Mol Med 2009; 15:510-8.
3. Ichinohe T, Maruya E, Saji H. Long-term fetal-maternal microchimerism: nature's hidden clue for alternative donor hematopoietic cell transplantation? Int J Hematol 2002; 76:229-37.
4. Bianchi DW, Zickwolf GK, Weil GJ, Sylvester S, DeMaria MA. Male fetal progenitor cells persist in maternal blood for as long as 27 years postpartum. Proc Natl Acad Sci USA 1996; 93:705-8.
5. Evans PC, Lambert N, Maloney S, Furst DER, Moore JM, Nelson JL. Long-term fetal microchimerism in peripheral blood mononuclear cell subsets in healthy women and women with scleroderma. Blood 1999; 93:2033-7.
6. Maloney S, Smith A, Furst DE, Myerson D, Rupert K, Evans PC, et al. Microchimerism of maternal origin persists into adult life. J Clin Invest 1999; 104:41-7.
7. Jonsson AM, Uzunel M, Götherström C, Papadogiannakis N, Westgren M. Maternal microchimerism in human fetal tissues. Am J Obstet Gynecol 2008; 198:3251-6.
8. Gadi VK, Nelson JL. Fetal microchimerism in women with breast cancer. Cancer Res 2007; 67:9035-8.
9. Cirello V, Perrino M, Colombo C, Muzza M, Filopanti M, Vincenti L, et al. Fetal cell microchimerism in papillary thyroid cancer: studies in peripheral blood and tissues. Int J Cancer 2010; 126:2874-8.
10. Stevens AM, Hermes HM, Rutledge JC, Buyon JP, Nelson JL. Myocardial-tissue-specific phenotype of maternal microchimerism in neonatal lupus congenital heart block. Lancet 2003; 362:1617-23.
11. Suskind DL, Rosenthal P, Heyman MB, Kong D, Magrane G, Baxter-Lowe LA, et al. Maternal microchimerism in the livers of patients with biliary atresia. BMC Gastroenterol 2004; 4:14.
12. Ichinohe T, Teshima T, Matsuoka K, Maruya E, Saji H. Fetal-maternal microchimerism: impact on hematopoietic stem cell transplantation. Curr Opin Immunol 2005; 17:546-52.
13. Tokita K, Terasaki P, Maruya E, Saji H. Tumour regression following stem cell infusion from daughter to microchimeric mother. Lancet 2001; 358:2047-8.
14. Ochiai N, Shimazaki C, Fuchida S, Okano A, Sumikuma T, Ashihara E, et al. Successful non-T cell-depleted HLA haploidentical three-loci mismatched hematopoietic stem cell transplantatioin from mother to son based on feto-maternal microchimerism in chronic myelogenous leukemia. Bone Marrow Transplant 2002; 30:793.
15. Wang Q, Zhu P. High doses of maternal lymphocyte infusions to treat EBV-associated lymphoma in pediatric patients. Blood 2009; 114:Abstract 785.
16. Zhang L, Miller RG. The correlation of prolonged survival of maternal skin grafts with the presence of naturally transferred maternal T cells. Transplantation 1993; 56:918-21.
17. Andrassy J, Kusaka S, Jankowska-Gan E, Torrealba JR, Marthaler BR, Tam RC, et al. Tolerance to noninherited maternal MHC antigens in mice. J Immunol 2003; 171:5554-61.
18. Mold JE, Michaelsson J, Burt TD, Muench MO, Beckerman KP, Busch MP, et al. Maternal alloantigens promote the development of tolerogenic fetal regulatory T cells in utero. Science 2008; 322:1562-5.
19. Matsuoka K, Ichinohe T, Hashimoto D, Asakura S, Tanimoto T, Teshima T, et al. Fetal tolerance to maternal antigens improves the outcome of allogeneic bone marrow transplantation by a $CD4^+CD25^+$ T-cell-dependent mechanism. Blood 2006; 107:404-9.
20. Aluvihare VR, Kallikourdis M, Bets AG. Regulatory T cells mediate maternal tolerance to the fetus. Nat Immunol 2004; 5:266-71.
21. Tamaki S, Ichinohe T, Matsuo K, Hamajima N, Hirabayashi N, Dohy H. Superior survival of blood and marrow stem cell recipients given maternal grafts over recipients given paternal grafts. Bone Marrow Transplant 2001; 28:375-80.
22. van Rood JJ, Loberiza FR Jr, Zhang MJ, Oudshoorn M, Claas F, Cairo MS, et al. Effect of tolerance to noninherited maternal antigens on the occurrence of graft-versus-host disease after bone marrow transplantation from a parent or an HLA-haploidentical sibling. Blood 2002; 99:1572-7.
23. Stern M, Ruggeri L, Mancusi A, Bernardo ME, de Angelis C, Bucher C, et al. Survival after T cell-depleted haploidentical stem cell transplantation is improved using the mother as donor. Blood 2008; 112:2990-5.
24. Ichinohe T, Uchiyama T, Shimazaki C, Matsuo K, Tamaki S, Hino M, et al. Feasibility of HLA-haploidentical hematopoietic stem cell transplantation between noninherited maternal antigen (NIMA)-mismatched family members linked with long-term fetomaternal microchimerism. Blood 2004; 104:3821-8.
25. Okumura H, Yamaguchi M, Kotani T, Sugimori N, Sugimori C, Ozaki J, et al. Graft rejection and hyperacute graft-versus-host disease in stem cell transplantation from non-inherited maternal antigen-complementary HLA-mismatched siblings. Eur J Haematol 2007; 78:157-60.
26. Kanda J, Ichinohe T, Shimazaki C, Hamaguchi M, Watanabe A, Ishida H, et al. Long-term survival after HLA-haploidentical SCT from noninherited maternal antigen-mismatched family donors: impact of chronic GVHD. Bone Marrow Transplant 2009; 44:327-9.
27. Cai J, Lee J, Jankowska-Gan E, Derks R, Pool J, Mutis T, et al. Minor H antigen HA-1-specific regulator and effector $CD8^+$ T cells and HA-1 microchimerism, in allograft tolerance. J Exp Med 2004; 199:1017-23.
28. van Halteren AG, Jankowska-Gan E, Joosten A, Blockland E, Pool J, Brand A, et al. Naturally acquired tolerance and sensitization to minor histocomaptibility antigens in healthy family donors. Blood 2009; 114:2263-72.
29. Dutta P, Molitor-Dart M, Bobadilla JL, Roenneburg DA, Yan Z, Torrealba JR, et al. Microchimerism is strongly correlated with tolerance to noninherited maternal antigens in mice. Blood 2009; 114:3578-87.
30. Molitor-Dart ML, Andrassy J, Haynes LD, Burlingham WJ. Tolerance induction or sensitization in mice exposed to noninherited maternal antigens (NIMA). Am J Transplant 2008; 8:2307-15.

Int J Hematol
DOI 10.1007/s12185-011-0820-0

ORIGINAL ARTICLE

Clinical significance of subcategory and severity of chronic graft-versus-host disease evaluated by National Institutes of Health consensus criteria

Takayuki Sato · Tatsuo Ichinohe · Junya Kanda · Kouhei Yamashita · Tadakazu Kondo · Takayuki Ishikawa · Takashi Uchiyama · Akifumi Takaori-Kondo

Received: 12 October 2010 / Revised: 21 February 2011 / Accepted: 16 March 2011

Abstract To evaluate the clinical significance of subcategory and severity of chronic graft-versus-host disease (GVHD) as defined by the National Institutes of Health (NIH) consensus criteria, we retrospectively studied 211 patients with hematologic neoplasms who survived beyond 100 days after allogeneic hematopoietic cell transplantation. Endpoints included chronic GVHD-specific survival (cGSS), duration of immunosuppressive treatment, and non-relapse mortality (NRM). A total of 96 patients fulfilled the NIH diagnostic criteria for cGVHD. In univariable analysis, patients with NIH overlap syndrome tended to exhibit lower cGSS compared to those with NIH classic cGVHD [hazard ratio (HR) = 2.76, $P = 0.060$], while patients with severe cGVHD at onset had a significantly lower cGSS compared to those with mild-to-moderate cGVHD (HR = 3.10, $P = 0.034$). The duration of immunosuppressive treatment was not significantly affected by either subcategory or severity of NIH cGVHD. In multivariable analysis treating cGVHD as a time-dependent covariate, development of overlap syndrome (HR = 3.90, $P = 0.014$) or severe cGVHD at peak worsening (HR = 6.21, $P < 0.001$) was significantly associated with higher risk of NRM compared to the absence of cGVHD. Our results suggest that both the subcategory and severity of NIH cGVHD are partly correlated with cGSS and may play a useful role in distinguishing patients at high risk for NRM, warranting validation of this approach through future prospective studies.

Keywords Hematopoietic cell transplantation · Chronic graft-versus-host disease · NIH consensus criteria

1 Introduction

Chronic graft-versus-host disease (cGVHD) remains a serious complication associated with substantial late morbidity and mortality after allogeneic hematopoietic cell transplantation (allo-HCT). In contrast to acute GVHD (aGVHD), which preferentially affects specific organs such as the skin, liver, and gastrointestinal tract, cGVHD presents with protean organ dysfunctions and various degrees of immunodeficiency that is further worsened by immunosuppressive medications used for relieving symptoms associated with GVHD [1]. Previous studies have identified a variety of factors that increase the risk of the development of cGVHD, including a prior history of aGVHD, older patient age, use of alloimmune female donors for male recipients, transplants from unrelated or human leukocyte antigen (HLA)-mismatched donors, and use of peripheral blood grafts [2–10]. In this context, clinical management of cGVHD has increasingly become more important, because recent trends in allo-HCT such as expanding applications of peripheral blood stem cell

A part of this study was presented as an abstract at the 51th Annual Meeting of American Society of Hematology, New Orleans, LA, USA, December 6, 2009.

T. Uchiyama: Deceased.

T. Sato · T. Ichinohe (✉) · J. Kanda · K. Yamashita · T. Kondo · T. Ishikawa · T. Uchiyama · A. Takaori-Kondo
Department of Hematology and Oncology,
Graduate School of Medicine, Kyoto University,
54 Shogoin Kawaharacho, Sakyo-ku, Kyoto 606-8507, Japan
e-mail: nohe@kuhp.kyoto-u.ac.jp

Present Address:
J. Kanda
Division of Cellular Therapy,
Duke University Medical Center, Durham, NC, USA

Published online: 05 April 2011

transplantation after reduced-intensity conditioning in older patients may increase the incidence of cGVHD [11].

Historically, aGVHD and cGVHD were distinguished based on whether immune-mediated organ dysfunction occurred within 100 days or more than 100 days after transplantation. However, accumulating experience has indicated that clinical manifestations similar to aGVHD can develop even several months after allo-HCT, while GVHD with typical features of the "chronic" form can occur as early as 2 months post-transplantation [12, 13]. Therefore, an arbitrary classification using the timing of GVHD onset is no longer considered appropriate. Another drawback in the management of cGVHD is that the grading criteria for its severity has not been standardized: it is difficult to predict the risk of GVHD-associated mortality by using historic classification that categorizes cGVHD into limited and extensive subtypes [14], because clinical severity as well as organ involvement of patients classified as having extensive cGVHD varies considerably [15–17].

To resolve these issues, the National Institutes of Health (NIH) consensus criteria were recently proposed to standardize the diagnosis and global assessment of cGVHD with a new severity scoring system based on organ-specific manifestations taking functional impact into account [18]. The NIH criteria distinguished two subcategories of cGVHD, "classic cGVHD" without features of aGVHD and "an overlap syndrome" in which characteristic features of both cGVHD and aGVHD are simultaneously present. In particular, features of aGVHD occurring beyond day 100 without manifestations of classic cGVHD are classified as "persistent", "recurrent", or "late-onset" aGVHD. Based on the number of involved organs and the severity within affected organs, each subcategory of cGVHD was graded into mild, moderate, or severe subtype. However, clinical significance of NIH cGVHD subcategory as well as their severity is not fully established, although several studies have shown their impact on overall survival, cGVHD-specific survival (cGSS), and non-relapse mortality (NRM) [19–23].

In the present study, we retrospectively evaluated patients who received allo-HCT for intractable hematologic disorders with special focus on the influences of subcategory and severity of NIH cGVHD on clinical outcomes. Since probabilities of GVHD-specific survival and discontinued immunosuppressive treatment (IST) have been most commonly used as surrogate endpoints representing the clinical resolution of cGVHD [24–26], we analyzed factors associated with these outcomes in patients who developed NIH cGVHD. We also evaluated the impact of the presence or absence of each subtype of NIH cGVHD on NRM.

2 Patients and methods

2.1 Patients

We retrospectively reviewed the medical records of 259 consecutive patients with hematologic disorders who underwent allo-HCT between January 2000 and December 2008 in our department and survived at least 100 days after transplantation. Patients were excluded if they had a history of previous allo-HCT ($n = 24$), rejected graft ($n = 4$), or relapsed before day 100 ($n = 20$); thus, a total of 211 patients were included in the present analysis. No patients received donor lymphocyte infusions before day 100. Patients with malignant hematologic neoplasms were defined as having standard-risk disease if they underwent transplantation in first complete remission or without prior chemotherapy, while those who underwent transplantation in any other status were classified as having high-risk disease. Patients with aplastic anemia were considered to have standard-risk disease. This study was approved by the Ethics Committee of Kyoto University Graduate School of Medicine. Written informed consent for the transplantation protocol was obtained from all patients.

2.2 Transplantation procedure

Patients with malignant hematologic neoplasms received myeloablative or fludarabine-based reduced-intensity conditioning regimens with or without total-body irradiation (TBI) as described elsewhere [27, 28]. Patients with aplastic anemia received conditioning regimens consisting of high-dose cyclophosphamide and horse or rabbit anti-lymphocyte globulin with or without 2–4 Gy TBI. None of these patients received T-cell-depleted grafts. All patients received GVHD prophylaxis by the use of cyclosporine or tacrolimus combined with or without short-term methotrexate. A proportion of patients given transplants from HLA-mismatched family members or unrelated marrow donors received mycophenolate mofetil in addition to tacrolimus plus methotrexate as GVHD prophylaxis [28]. All patients received supportive care including blood product transfusion and prophylaxis against opportunistic infections according to our institutional protocols [29].

2.3 Evaluation and management of acute and chronic GVHD

All patients were graded for aGVHD using conventional criteria, and the maximum grade until day 100 after transplantation was assigned [30]. Patients who developed grade II–IV aGVHD were initially treated with methylprednisolone or prednisolone usually at a dose of 1–2 mg/kg. Treatment of steroid-refractory aGVHD was variable.

The incidence of cGVHD was retrospectively evaluated by using the NIH consensus criteria [18]. Patients who had at least one "diagnostic" clinical sign or at least one "distinctive" manifestation, confirmed by relevant laboratory tests or histologic examination, were defined as having cGVHD if other possible diagnoses were excluded. Subclassification of cGVHD into "classic cGVHD" and "overlap syndrome" was strictly according to the NIH criteria. If patients had any features of aGVHD along with classic cGVHD, they were classified as having an overlap syndrome. The severity of cGVHD was assessed at its onset and at maximal clinical worsening and graded into "mild", "moderate", and "severe" categories according to the global scoring system defined by the NIH criteria. Treatment of cGVHD was variable, but followed some general principles; patients with isolated mouth, ocular, or localized skin cGVHD were treated only with topical therapy, while patients with more symptomatic cGVHD were treated with systemic immunosuppressive agents such as prednisolone at a dose of 0.5–1.0 mg/kg per day combined with calcineurin inhibitors. Although the duration and dosing of those agents were not standardized, patients typically received treatment until all symptoms of cGVHD were resolved or stabilized. Patients with less severe symptoms were often treated with peroral low-dose prednisolone at a dose of less than 0.5 mg/kg per day.

2.4 Statistical analysis

Descriptive statistics were used to summarize variables related to patient and transplant characteristics. Comparisons among the groups were performed by use of extended Fisher exact test for categorical variables and Wilcoxon–Mann–Whitney test for continuous variables. The primary endpoint of the study was cGSS, which is defined as the time from the day of diagnosis of cGVHD to the day of death in the absence of relapse or secondary malignancy, among patients who developed NIH cGVHD stratified by its subcategory or severity at onset. The probabilities of cGSS were estimated according to the Kaplan–Meier method, and univariable comparison between groups was made using the log-rank test. Patients who were alive without recurrent or secondary malignancy were censored at their last follow-up visit and those who experienced recurrent or secondary malignancy were censored at the time of its diagnosis. The time to discontinuation of IST was defined among patients who received systemic IST for the treatment of NIH cGVHD as the time from the day of diagnosis of cGVHD to the day of withdrawal of systemic IST. NRM was defined among all patients included in the study as rates of death without evidence of primary disease recurrence. The incidence rates of IST withdrawal and those of NRM were estimated with the use of the cumulative incidence method to accommodate the following competing events [31]: the onset of recurrent or secondary malignancy and death from any cause for IST withdrawal, and the recurrent primary disease for NRM. Cox proportional-hazards regression models were used to evaluate variables potentially associated with cGSS, while competing risks regression models were used to evaluate variables potentially associated with IST withdrawal and NRM [32]. The variables included in the analysis were as follows: patient age, donor–recipient sex combination, disease status at the time of transplantation, donor–recipient HLA compatibility, stem cell sources, type of conditioning regimens, grades of prior aGVHD (grades 0–1 vs. grades 2–4), subcategory of NIH cGVHD (classic cGVHD vs. overlap syndrome), global severity of NIH cGVHD at onset (mild to moderate vs. severe), platelet counts, eosinophil counts, and administration of systemic corticosteroids at the onset of cGVHD. In the analysis to evaluate the impact of the presence of each NIH cGVHD subtype on NRM for the entire cohort of patients in the study, development of each subtype of cGVHD was treated as a time-dependent covariate under the assumption that a patient who developed moderate or severe cGVHD could not revert to less severe cGVHD and that classic cGVHD and overlap syndrome could not switch to each other [33]. Factors having two-sided P values less than 0.1 for association with outcome were included in multivariable model using a forward and backward stepwise method with a predetermined risk of 0.1. Two-sided P values <0.05 were considered to be statistically significant. All analyses were performed using STATA version 11 (College Station, TX, USA) according to patient information available as of 1 July 2009.

3 Results

3.1 Patient characteristics

Table 1 shows the characteristics of the 211 patients included in the study; they had a median age of 46 years, included 113 males and 98 females, and underwent transplantation for malignant hematologic neoplasms in most cases. The number of patients who received bone marrow, peripheral blood, and cord blood unit was 152 (72%), 44 (21%), and 15 (7%), respectively. After a median follow-up of 37.2 months (range 3.3–111.6), a total of 96 patients (45%) developed manifestations of cGVHD that met the NIH consensus criteria. There was no statistically significant difference in background characteristics between patients who developed NIH cGVHD and those who did not, except that the former group included higher proportion of patients with a history of antecedent grade II–IV aGVHD.

Table 1 Patient and transplantation characteristics

Characteristic	All patients ($n = 211$)	NIH cGVHD		
		Absent ($n = 115$)	Present ($n = 96$)	P value
Median patient age, years (range)	46 (17–69)	46 (19–69)	47 (17–67)	0.90
Donor/recipient sex combination, *n* (%)				0.17
Male/male	66 (31)	41 (35)	25 (26)	
Male/female	42 (20)	21 (18)	21 (22)	
Female/female	56 (27)	33 (29)	23 (24)	
Female/male	47 (22)	20 (17)	27 (28)	
Diagnosis, *n* (%)				0.59
Myeloid neoplasms	113 (54)	65 (57)	48 (50)	
Precursor lymphoid neoplasms	31 (15)	17 (15)	14 (15)	
Mature lymphoid neoplasms	61 (29)	29 (25)	32 (33)	
Aplastic anemia	6 (3)	4 (3)	2 (2)	
Disease status at transplant, *n* (%)				0.41
Standard risk	105 (50)	54 (47)	51 (53)	
High risk	106 (50)	61 (53)	45 (47)	
Donor type[a], *n* (%)				0.71
HLA-matched related	83 (39)	45 (39)	38 (40)	
HLA-mismatched related	23 (11)	12 (10)	11 (11)	
HLA-matched unrelated	89 (42)	47 (41)	42 (44)	
HLA-mismatched unrelated	16 (8)	11 (10)	5 (5)	
Donor/recipient HLA compatibility[a], *n* (%)				0.59
Matched	172 (82)	92 (80)	80 (83)	
Mismatched	39 (18)	23 (20)	16 (17)	
Stem cell source, *n* (%)				0.30
Bone marrow	152 (72)	85 (74)	67 (70)	
Peripheral blood	44 (21)	20 (17)	24 (25)	
Cord blood	15 (7)	10 (9)	5 (5)	
Conditioning regimen, *n* (%)				0.55
Myeloablative with TBI	113 (54)	64 (56)	49 (51)	
Myeloablative without TBI	15 (7)	10 (9)	5 (5)	
Reduced intensity with TBI	65 (31)	33 (29)	32 (33)	
Reduced intensity without TBI	18 (9)	8 (7)	10 (10)	
GVHD prophylaxis, *n* (%)				0.73
Tacrolimus based	169 (80)	91 (79)	78 (81)	
Cyclosporine based	42 (20)	24 (21)	18 (19)	
Prior aGVHD, *n* (%)				0.048
Grade 0–1	117 (55)	70 (61)	47 (49)	
Grade 2	72 (34)	38 (33)	34 (35)	
Grade 3–4	22 (10)	7 (6)	15 (16)	
Median months (range) after transplantation[b]	37.2 (3.3–111.6)	35.6 (3.3–111.6)	40.6 (4.0–105.3)	0.14

cGVHD chronic graft-versus-host disease, *aGVHD* acute graft-versus-host disease, *TBI* total-body irradiation

[a] HLA matching was defined by 2-digit compatibility at HLA-A, -B, and -DRB1 loci

[b] Median follow-up months among patients who were alive at the time of last follow-up

Table 2 summarizes the characteristics of 96 patients who developed NIH cGVHD according to its subcategory; 77 (80%) developed "classic cGVHD" and 19 (20%) developed "overlap syndrome". A total of 31 (40%) patients with classic GVHD and 18 (95%) with overlap syndrome had a prior history of grade II–IV aGVHD. The

median time from transplantation to the onset of cGVHD in patients with overlap syndrome was shorter compared to patients with classic cGVHD (4.1 vs. 7.1 months, $P < 0.001$). All patients with overlap syndrome were graded as having moderate or severe cGVHD, whereas the proportion of patients who developed severe cGVHD was similar between patients with classic cGVHD and those with overlap syndrome. Proportions of patients with platelet counts less than $100 \times 10^3/\mu L$, eosinophil counts less than $500/\mu L$, and ongoing systemic corticosteroid treatment at the onset of cGVHD were higher among patients who developed overlap syndrome compared with those who developed classic cGVHD.

3.2 Chronic GVHD-specific survival

Of the 96 patients who developed NIH cGVHD, recurrent or secondary malignant neoplasm occurred in 27 patients and death due to any cause occurred in 31 patients. The respective 3-year probabilities of cGSS among patients who developed classic cGVHD and overlap syndrome were 88 and 70% ($P = 0.060$) (Fig. 1a), while those among subgroups of patients graded to have mild, moderate, and severe cGVHD at onset were 100, 86, and 69% (mild to moderate vs. severe, $P = 0.034$) (Fig. 1b). Table 3 shows the results of univariable and multivariable analyses for factors potentially associated with cGSS among the patients who developed NIH cGVHD. In univariable analysis, the presence of severe cGVHD and thrombocytopenia at cGVHD onset were significantly associated with lower cGSS, whereas the presence of an overlap syndrome and high-risk malignant disease tended to be associated with lower cGSS. In multivariable analysis, the presence of thrombocytopenia at cGVHD onset was the only significant factor that adversely affected cGSS [hazard ratio (HR) for mortality = 4.05, 95% confidence interval (CI) = 1.35–12.1, $P = 0.013$], although patients with severe cGVHD (HR = 2.58, 95% CI = 0.90–7.39, $P = 0.077$) or those with high-risk underlying disease (HR = 2.75, 95% CI = 0.86–8.80, $P = 0.088$) also had a trend toward lower cGSS.

3.3 Duration of systemic immunosuppressive treatment

A total of 81 patients received systemic immunosuppressive agents for the treatment of NIH cGVHD. In this group of patients, the cumulative incidence of withdrawal of systemic IST was 40% (95% CI = 29–51%) at 3 years after the onset of cGVHD, while the cumulative incidence of the competing risks of death or recurrent/secondary malignancy during systemic IST was 42% (95% CI = 32–55%) (Fig. 2). In univariable analysis, no significant association was found between discontinuation of IST and subcategory or global severity of NIH cGVHD (overlap syndrome vs. classic cGVHD, HR for IST withdrawal = 0.51, 95% CI = 0.20–1.31, $P = 0.16$; severe vs. mild to moderate, HR = 0.90, 95% CI = 0.42–1.96, $P = 0.80$). Multivariable analysis revealed two factors significantly associated with prolonged administration of systemic IST; high-risk primary disease (HR = 0.39, 95% CI = 0.19–0.77, $P = 0.007$) and the ongoing use of systemic corticosteroids at the onset of cGVHD (HR = 0.40, 95% CI = 0.19–0.84, $P = 0.015$).

3.4 Non-relapse mortality

Death from non-relapse causes occurred in 16 (17%) of 96 patients who developed NIH cGVHD and in 10 (9%) of 115 patients who did not. In a multivariable analysis of the entire series of 211 patients, treating the subcategory or peak severity of NIH cGVHD as a time-dependent covariate, development of the overlap syndrome or severe cGVHD was significantly associated with higher risk of NRM compared to the absence of cGVHD (overlap syndrome vs. no cGVHD, HR = 3.90, 95% CI = 1.32–11.6, $P = 0.014$; severe cGVHD vs. no cGVHD, HR = 6.21, 95% CI = 2.25–17.1, $P < 0.001$). Development of classic cGVHD or mild-to-moderate cGVHD was not significantly associated with higher risk of NRM when compared with the absence of NIH cGVHD (classic cGVHD vs. no cGVHD, HR for mortality = 1.39, 95% CI = 0.55–3.53, $P = 0.49$; mild-to-moderate cGVHD vs. no cGVHD, HR = 2.25, 95% CI = 0.62–8.18, $P = 0.22$).

4 Discussion

In the present study, we evaluated the clinical significance of subcategory and severity of NIH cGVHD in terms of their influences on cGSS, discontinuation of IST, and NRM using a retrospective cohort of patients who underwent allo-HCT for hematologic disorders. In univariable analysis, patients with overlap syndrome tended to have a lower probability of cGSS than those with classic cGVHD, while patients who developed severe cGVHD had significantly worse cGSS compared with those who developed mild-to-moderate cGVHD. Although such differences in cGSS according to NIH cGVHD subtypes did not reach statistical significance by multivariable analysis, patients who developed overlap syndrome or severe NIH cGVHD had a significantly higher NRM than those who did not develop any manifestation of NIH cGVHD. These results suggest that both subcategory and global severity of NIH cGVHD might be useful for evaluating the risk of GVHD-associated mortality in patients diagnosed to have cGVHD by the NIH criteria. In

Table 2 Characteristics of chronic GVHD according to subcategory defined by the National Institutes of Health criteria

Characteristics	Total ($n = 96$)	NIH cGVHD subcategory		
		Classic cGVHD ($n = 77$)	Overlap syndrome ($n = 19$)	P value
Median months (range) to onset of cGVHD	6.7 (2.1–29.9)	7.1 (2.7–29.9)	4.1 (2.1–20.7)	<0.001
Involved organs or sites[a], n (%)[b]				0.92
Skin	55 (57)	40 (52)	15 (79)	
Mouth	69 (72)	56 (73)	13 (68)	
Eyes	29 (30)	23 (30)	6 (32)	
Gastrointestinal tract	34 (35)	25 (32)	9 (47)	
Liver	76 (79)	61 (79)	15 (79)	
Lungs	12 (12)	9 (12)	3 (16)	
Joints and fascia	4 (4)	3 (4)	1 (5)	
Genital tract	2 (2)	2 (3)	0 (0)	
Number of involved organs or sites[a], n (%)				0.14
1	7 (7)	7 (9)	0 (0)	
2	27 (28)	24 (31)	3 (16)	
3 or more	62 (65)	46 (60)	16 (84)	
Maximum score of involved organs[a], n (%)				0.18
Score 1	22 (23)	20 (26)	2 (11)	
Score 2 (other than lungs)	26 (27)	18 (62)	8 (42)	
Score 2 (lungs)	6 (6)	4 (5)	2 (11)	
Score 3	42 (44)	35 (45)	7 (37)	
Severity at onset, n (%)				0.023
Mild	20 (21)	20 (26)	0 (0)	
Moderate	53 (55)	39 (51)	14 (74)	
Severe	23 (24)	18 (23)	5 (26)	
Severity at peak, n (%)				0.17
Mild	12 (13)	12 (16)	0 (0)	
Moderate	39 (41)	29 (38)	10 (53)	
Severe	45 (47)	36 (47)	9 (47)	
Platelet count at cGVHD onset, n (%)				0.002
$100 \times 10^3/\mu L$ or more	65 (68)	58 (75)	7 (37)	
Less than $100 \times 10^3/\mu L$	31 (32)	19 (25)	12 (63)	
Eosinophil count at cGVHD onset, n (%)				0.010
Less than 500/μL	68 (71)	50 (65)	18 (95)	
500/μL or more	28 (29)	27 (35)	1 (5)	
Systemic corticosteroids at cGVHD onset, n (%)				<0.001
Not received	63 (66)	61 (79)	2 (11)	
Received	33 (34)	16 (21)	17 (89)	

cGVHD chronic graft-versus-host disease

[a] Data evaluated at peak clinical worsening are shown

[b] The sum of the number per involved site is not equal to the number of evaluable patients, because the involvement of more than one organ can occur in a single patient. Accordingly, the sum of percentage among the total number of patients does not equal to one hundred

contrast, duration of IST was neither affected by NIH cGVHD subcategory nor by its severity.

While cGSS has been frequently used as a study endpoint to describe the mortality attributable to cGVHD-associated organ dysfunction, there have been no established early surrogates that help to guide the clinical management of patients with evidence of ongoing cGVHD. Given that the historic limited/extensive grading system is not a useful predictor for the severity of organ involvement in terms of mortality risk, several studies have attempted to develop